

BRL MR 2762

BRL



ADA 042025

MEMORANDUM REPORT NO. 2762

MEASUREMENTS ON A CIRCULAR PLATE
IMMERSED IN MUZZLE FLOW

Edmund J. Gion
Edward M. Schmidt

June 1977

Approved for public release; distribution unlimited.



AD NO. 1
DDC FILE COPY

USA ARMAMENT RESEARCH AND DEVELOPMENT COMMAND
USA BALLISTIC RESEARCH LABORATORY
ABERDEEN PROVING GROUND, MARYLAND

Destroy this report when it is no longer needed.
Do not return it to the originator.

Secondary distribution of this report by originating
or sponsoring activity is prohibited.

Additional copies of this report may be obtained
from the National Technical Information Service,
U.S. Department of Commerce, Springfield, Virginia
22151.

The findings in this report are not to be construed as
an official Department of the Army position, unless
so designated by other authorized documents.

*The use of trade names or manufacturers' names in this report
does not constitute indorsement of any commercial product.*

UNCLASSIFIED

SECURITY CLASSIFICATION OF THIS PAGE (When Data Entered)

REPORT DOCUMENTATION PAGE		READ INSTRUCTIONS BEFORE COMPLETING FORM
1. REPORT NUMBER BRL Memorandum Report No. 2762	2. GOVT ACCESSION NO.	3. RECIPIENT'S CATALOG NUMBER
4. TITLE (and Subtitle) MEASUREMENTS ON A CIRCULAR PLATE IMMersed IN MUZZLE FLOW,	5. TYPE OF REPORT & PERIOD COVERED Final report	
6. AUTHOR(s) Edmund J. Gion and Edward M. Schmidt	7. PERFORMING ORG. REPORT NUMBER	
8. PERFORMING ORGANIZATION NAME AND ADDRESS USA Ballistic Research Laboratory Aberdeen Proving Ground, Maryland 21005	9. CONTRACT OR GRANT NUMBER(s)	
10. CONTROLLING OFFICE NAME AND ADDRESS US Army Materiel Development & Readiness Command 5001 Eisenhower Avenue Alexandria, Virginia 22333	11. PROGRAM ELEMENT, PROJECT, TASK AREA & WORK UNIT NUMBERS RDT&E 11L662618A180	
12. MONITORING AGENCY NAME & ADDRESS (if different from Controlling Office) 37p.	13. REPORT DATE JUNE 1977	
	14. NUMBER OF PAGES 45	
	15. SECURITY CLASS. (of this report) UNCLASSIFIED	
	16. DECLASSIFICATION/DOWNGRADING SCHEDULE	
17. DISTRIBUTION STATEMENT (of this Report) Approved for public release; distribution unlimited EPI-MR-2762		
18. DISTRIBUTION STATEMENT (for the Abstract entered in Block 20, if different from Report)		
19. SUPPLEMENTARY NOTES		
20. KEY WORDS (Continue on reverse side if necessary and identify by block number) Muzzle blast Muzzle brake Pressure blast		
21. ABSTRACT (Continue on reverse side if necessary and identify by block number) (ner) Results are given of pressure measurements on the surface of a simplistic muzzle brake for a 20mm gun. The pressure variations for about 400µs after shot ejection were obtained for a number of axial brake locations. Peak overpressure and "steady-state" overpressure levels are presented; the steady-state values are compared with theory and agreement is good.		

039 4.9

1/B

TABLE OF CONTENTS

	Page
LIST OF ILLUSTRATIONS	3
I. INTRODUCTION	5
II. INSTRUMENTATION AND TEST PROCEDURE	7
III. RESULTS	8
IV. CONCLUSIONS12
ACKNOWLEDGMENTS12
LIST OF REFERENCES36
LIST OF SYMBOLS38
DISTRIBUTION LIST39

ACCESSION for	
NTIS	Write Section <input checked="" type="checkbox"/>
DDC	Buff Section <input type="checkbox"/>
UNANNOUNCED	<input type="checkbox"/>
JUSTIFICATION	
BY	
DISTRIBUTION/AVAILABILITY CODES	
Dist.	AVAIL. and/or SPECIAL
A	

DDC
RECEIVED
 JUL 27 1977
RECEIVED
 D

PRECEDING PAGE BLANK-NOT FILMED

LIST OF ILLUSTRATIONS

Figure	Page
1a. Photograph of Double Baffle Muzzle Brake for 155mm Gun . . .	13
1b. Schematic of Sabot Deflector	14
1c. Schematic of Silencer	14
2. Muzzle Flow Field	15
3. Photographs of Test Set-up	16
4. Schematic of Test Set-up	17
5a. Pressures on Muzzle Brake at Various Radial Locations, $[\bar{p} = (p-p_{\infty})/p_{\infty}]$, $X/D = 0.5$	18
5b. Pressures on Muzzle Brake at Various Radial Locations, $[\bar{p} = (p-p_{\infty})/p_{\infty}]$, $X/D = 1.0$	19
5c. Pressures on Muzzle Brake at Various Radial Locations, $[\bar{p} = (p-p_{\infty})/p_{\infty}]$, $X/D = 1.5$	20
5d. Pressures on Muzzle Brake at Various Radial Locations, $[\bar{p} = (p-p_{\infty})/p_{\infty}]$, $X/D = 2.0$	21
5e. Pressures on Muzzle Brake at Various Radial Locations, $[\bar{p} = (p-p_{\infty})/p_{\infty}]$, $X/D = 4.0$	22
5f. Pressures on Muzzle Brake at Various Radial Locations, $[\bar{p} = (p-p_{\infty})/p_{\infty}]$, $X/D = 6.0$	23
5g. Pressures on Muzzle Brake at Various Radial Locations, $[\bar{p} = (p-p_{\infty})/p_{\infty}]$, $X/D = 8.0$	24
6. Spark Shadowgraphs of Flow over Muzzle Brake Located at $X/D = 6.0$	25
7. Maximum and Steady State Pressures on Muzzle Brake Surface: a. $X/D = 0.5$; b. $X/D = 1.0$	28
Maximum and Steady State Pressures on Muzzle Brake Surface: c. $X/D = 1.5$	29
Maximum and Steady State Pressures on Muzzle Brake Surface: d. $X/D = 2.0$; e. $X/D = 4.0$	30
Maximum and Steady State Pressures on Muzzle Brake Surface: f. $X/D = 6.0$; g. $X/D = 8.0$	31

LIST OF ILLUSTRATIONS (Continued)

Figure		Page
8.	Schematic of Muzzle Brake in a Radial Flow Field	32
9.	Comparison of Steady Jet Theory with Present Data . . .	33
10.	Comparison of Surface Pressure Distribution with Theory of Smith	34
11.	Incremental Force Versus Brake Radius for $X/D = 1.0$. .	35

I. INTRODUCTION

The geometry of muzzle devices varies with the particular application of interest; however, a baffle placed perpendicular to the flow axis is common to a number of practical configurations. The muzzle brake, typified in Figure 1a, consists of a series of such baffles which utilize the momentum of the exhausting propellant gases to generate a counter-recoil force. Having a similarity to muzzle brakes, Figure 1b, sabot deflectors intercept sabot fragments very close to the muzzle thereby reducing the hazard to friendly operations. Blast suppressors and silencers, Figure 1c, are designed with a series of baffled compartments permitting internal expansion of the propellant gases prior to ejection into the atmosphere. Due to the necessity of attaching the muzzle device to the weapon, its geometry is not always axially symmetric. Obviously, the struts on the upper and lower surfaces of the muzzle brake, Figure 1a, destroy the symmetry of the baffle; however, the blast suppressor baffles are contained in a cylindrical housing and maintain symmetry. The present report describes the results of a test program on a circular plate placed in the muzzle flow of a 20mm gun. While this test bed is highly simplistic, it provides a representation of the basic baffle concept which is both experimentally and theoretically attractive.

Oswatitsch¹ and Smith^{2,3} consider axially symmetric baffles simulating muzzle brakes. Their analyses assume that the muzzle exhaust flow impinging on the baffle may be treated in a quasi-steady manner. This approximation is valid^{4,5} in describing properties

-
1. K. Oswatitsch, "Flow Research to Improve the Efficiency of Muzzle Brakes, Parts I-III," in *Muzzle Brakes, Volume II: Theory*, E. Hammer (ed.), Franklin Institute, Philadelphia, PA, 1949.
 2. F. Smith, "Model Experiments on Muzzle Brakes," RARDE R 2/66, Royal Armament Research and Development Establishment, Fort Halstead, U.K., 1966. AD 487 121.
 3. F. Smith, "Model Experiments on Muzzle Brakes, Part III: Measurement of Pressure Distribution," RARDE R 3/68, Royal Armament Research and Development Establishment, Fort Halstead, U.K., 1968. AD 845 519.
 4. E. M. Schmidt and D. D. Shear, "Optical Measurements of Muzzle Blast," *AIAA J.*, Vol. 13, No. 8, August 1975, pp. 1086-1091.
 5. K. Oswatitsch, "Intermediate Ballistics," DVL R 358, Deutschen Versuchsanstalt für Luft- und Raumfahrt, Aachen, Germany, June 1964. AD 473 249.

within the supersonic core of the propellant gas jet, Figure 2. Since the muzzle device is immersed in the core flow over most of its period of effectiveness, the results of quasi-steady analyses agree with gross measurements of recoil reduction obtained in ballistic pendulums. This approach has a serious shortcoming in that no information is provided on conditions within the shock layer. Since maximum gas-dynamic loadings are generated by impingement of the blast wave upon baffle surfaces, the unsteady processes must be addressed in designing for the ultimate strength of the device.

6-8

Recently, investigators have applied numerical techniques to the calculation of the time-dependent muzzle flow. Their results agree qualitatively with the limited data available describing the free field muzzle blast development. Some extensions^{9,10} of these approaches have been attempted to examine the flow over muzzle devices; however, since the models are currently restricted to the treatment of two-dimensional (axisymmetric) flow fields, the muzzle devices considered are simple, unsupported baffles placed in the flow. The similarity between the computational and present test geometries is obvious.

This report describes an experimental program conducted on a muzzle brake on a 20mm gun. To provide data for comparison with numerical models, the muzzle brake is restricted to a highly simplistic, axially symmetric geometry. Both optical and pressure measurements

-
6. R. M. Traci, J. L. Farr, and C. Y. Liu, "A Numerical Method for the Simulation of Muzzle Gas Flows with Fixed and Moving Boundaries," BRL CR 161, U. S. Army Ballistic Research Laboratory, Aberdeen Proving Ground, MD, June 1974. AD 784144.
 7. F. H. Maille, "Numerical Calculation of a 105mm Gun Blast with Projectile," NWL TR 3002, U. S. Naval Weapons Laboratory, Dahlgren, VA, August 1973. AD 770818.
 8. T. D. Taylor, "Calculation of Muzzle Blast Fields," PA R 4155, Picatinny Arsenal, Dover, NJ, December 1970. AD 881523L.
 9. C. K. Zoltani, "Calculation of the Muzzle Flow Field of the 155mm Howitzer M-109," BRL R 1901, U. S. Army Ballistic Research Laboratory, Aberdeen Proving Ground, MD, August 1976. AD B012935L.
 10. F. H. Maille, "Finite Difference Calculations of the Free-Air Blast Field About the Muzzle and a Simple Muzzle Brake of a 105mm Howitzer," NWL TR 2938, U. S. Naval Weapons Laboratory, Dahlgren, VA, May 1973.

were taken of the initial, highly unsteady flow and the subsequent relaxation to quasi-steady conditions. The latter data are used to examine the applicability of the steady flow approximations¹⁻³ to a real gun environment.

II. INSTRUMENTATION AND TEST PROCEDURE

The test set-up is shown in Figures 3 and 4. The weapon used in these experiments is a 20mm cannon which had previously undergone extensive testing to measure its muzzle exit conditions¹¹. To maintain the symmetry of the flow, the muzzle brake is a circular steel plate mounted separately from the gun but aligned with its axis of symmetry coincident to gun axis. Both the gun and brake are rigidly mounted in order to maintain their relative geometry during the firing process.

The gun has a barrel length of 1.52m, a chamber volume of $4.17 \times 10^{-5} \text{ m}^3$, and a twist of rifling of one turn in 25 calibers. The projectile is an M55A2 training round weighing 0.098 kg and having a length of 3.75 calibers. A charge of 0.0178 kg of WC870 propellant is used to launch the projectile at a velocity of 610 m/s. The propellant gas properties behind the projectile just prior to shot ejection are measured¹¹ to be

$$u_1 = 610 \text{ m/s}$$

$$a_1 = 700 \text{ m/s}$$

$$p/p_\infty = 127$$

This flow is subsonic; thus, at shot ejection, an expansion wave propagates back up the gun tube accelerating the propellant gases to a sonic exit condition:

$$u^* = a^* = 691 \text{ m/s}$$

$$p^*/p_\infty = 111$$

The muzzle brake is fabricated from steel, has a thickness of 0.031m, and a diameter of 0.457m. To permit passage of the projectile, a 24mm hole is machined at the center of the plate. Six pressure taps

11. E. M. Schmidt, E. J. Gion, and D. D. Shear, "Acoustic Thermometric Measurements of Propellant Gas Temperatures in Guns," *AIAA J.*, Vol. 15, No. 2, February 1977, pp. 222-226.

are located along a radial line on the brake surface. The first gauge is 20mm from the axis of symmetry, and the others are set at 10mm intervals. The pressure gauges are Kistler 603A and 201B piezoelectric transducers. Signals are recorded on Tektronix, type 551, dual beam oscilloscopes. The flow field development along the brake surface is recorded using a spark shadowgraph technique⁴. The position-time history of the projectile is measured using two X-ray photography stations located immediately downrange of the muzzle brake. The X-ray data are used to relate all of the results to a common time base, i.e., time zero is defined as occurring when the projectile obturator (located 9mm forward of the base) crosses the muzzle exit plane.

III. RESULTS

Plots of overpressure versus time for seven axial locations ($0.5 \leq X/D \leq 8.0$) of the muzzle brake are presented in Figures 5a-5g. The general properties of the traces are similar. The initial rapid increase in pressure is interpreted as corresponding to the arrival and reflection of the air blast at the particular station. Continued expansion of the blast along the brake surface and back into the muzzle jet permits the pressure level to decay from the peak reflected value. During this period of decay, the propellant gas flow arrives at the brake surface. The propellant gases are deflected by the brake and forced either to expand radially outward along the plate or to flow inward and exit through the projectile hole. The highly transient portion of this process lasts only for 50-100 microseconds, after which the pressure levels reach and maintain a "steady-state" value. This corresponds to the establishment of a quasi-steady propellant gas flow field over the muzzle brake. Changes in this flow occur relatively slowly as the gun tube empties.

Spark shadowgraphs of the muzzle flow for firings at a brake station of $X/D = 6.0$ are presented in Figure 6. Interaction between the precursor flow* and the propellant gas flow is clearly indicated, Figure 6b. This permits the propellant gases to accelerate rapidly in the forward direction due to the existence of an established flow field. As a result, the air blast is not spherical but has a bubble or bulge to the front. At certain gauge stations, arrival of this bifurcated shock would produce multiple pressure pulses. Additionally, the propellant gas flow following this blast is seen to be quite complex. A strong shock is formed at the base of the projectile. This shock follows the round up to the plate surface. The lateral or "barrel" shock structure of the propellant gas jet are of a mixed type, with both weak and strong oblique shocks being apparent. As the flow processed by these different shocks passes a given station, rapid changes in local flow conditions would be anticipated. Unfortunately,

*This is the flow field established when the air in the gun tube ahead of the projectile is forced out prior to shot ejection.

only a single photograph was taken of each firing; therefore, it is not possible to make an exact comparison between observed discontinuities in the shadowgraphs and measured pressure pulses. However, the various flow features shown in Figure 6 indicate that some of the wiggles in the pressure data are real.

Two values of pressure are of particular interest, the maximum pressure, p_m , and the steady state pressure, p_s , Figures 7a-7g. Both show similar variations with muzzle brake and gauge location. At a given axial location of the brake, there is an obvious decay of pressure in the radial direction. The radial pressure decay occurs more rapidly for brake positions near the muzzle than further out. This is due to the relative geometry of the flow fields and the plate. Both the blast and propellant gas jet tend to be roughly spherically symmetric^{4,12}, while the plate is a planar surface intercepting radials of this flow as shown in a sectional view, Figure 8. Using a Newtonian approximation¹³ leads to a $\cos^2\theta$ variation of the surface pressure, where θ is the angle between a normal to the plate surface and a flow radial. For a plate of height h the variation of $\cos^2\theta$ across the face of the plate is

$$1.0 \geq \cos^2 \theta \geq 1/(1 + \frac{h^2}{X^2}),$$

and is shown in the lower part of Figure 8. Near the muzzle, the range in h/X and $\cos^2\theta$ is large, e.g., for

$$X/D = 1.0,$$

$$1.0 \leq h/X \leq 3.5,$$

$$0.5 \geq \cos^2 \theta \geq 0.075.$$

However, further from the weapon, this is no longer true, e.g., for

$$X/D = 8.0,$$

$$0.125 \leq h/X \leq 0.438,$$

$$0.985 \geq \cos^2 \theta \geq 0.839.$$

-
12. J. I. Erdos and P. Del Guidice, "Calculation of Muzzle Blast Flow-fields," *AIAA J.*, Vol. 13, No. 8, August 1975, pp. 1048-1055.
 13. D. W. Eastman and L. P. Radtke, "Flow Field of an Exhaust Plume Impinging on a Simulated Lunar Surface," *AIAA J.*, Vol. 1, No. 6, June 1963, pp. 1430-1431.

This type of behavior is reflected in the measured pressure variations.

In examining the radial variation of steady state pressure, it is interesting to note that for axial brake locations of $0.5 \leq X/D \leq 2.0$, the plate surface pressure drops below atmospheric pressure. Similar behavior has been observed in steady jets impinging upon planar surfaces^{14,15}. This pressure decay is due to radial expansion of the deflected propellant gases. Carling and Hunt¹⁴ indicate the flow along the surface is accelerated to supersonic conditions, overexpands to sub-atmospheric conditions, and experiences pressure recovery through a series of shock waves. In the present data, overexpansion is observed; however, the radial extent of pressure transducers was not sufficient to detect shock recovery to ambient pressure levels. For practical applications, the outermost limit of transducers, $r/D = 3.5$, is beyond the extreme dimensions of most real muzzle brakes. While weight restricts the size of actual muzzle devices, the present data indicate an additional dimensional constraint due to the flow behavior: increased size could produce reduced efficiency due to overexpansion of the flow within the brake. This point was noted by Oswatitsch¹ in his analysis of optimum brake design.

At $X/D = 6.0$ and 8.0 , Figures 7f and 7g, the maximum pressure profiles across the plate do not show monotonic decay with radial location. This behavior is interpreted as arising from precursor-propellant gas interaction. As discussed previously, the main blast wave develops a "bubble" in the downrange direction. Near the axis of symmetry, the bubble reflects from the plate. Further away, the main blast is reflected and appears as the secondary increase in surface pressure (at $r/D = 2.0$ in both plots). For muzzle brake stations closer to the muzzle, the shock bubble has not formed and only the main blast is observed.

Both p_m and p_s reach peak values for brake axial locations between $1.0 < X/D < 2.0$. Further increase in X/D results in a steady decay of both pressure levels. Again, this is due to radial expansion of the flow and agrees with both blast and jet theories. To illustrate this agreement, consider the variation in p_s : In Figure 9 steady state pressure at the first gauge station, $r/D = 1.0$, is plotted against X/D . The measurements are compared with the

14. J. C. Carling and B. L. Hunt, "The Near Wall Jet of a Normally Impinging, Uniform, Axisymmetric, Supersonic Jet," *JFM*, Vol. 66, Part 1, 1974, pp. 159-176.

15. S. Hoffman, "Normal Impingement Loads due to Small Air Jets Issuing from a Base Plate," NASA, TN D 6817, June 1972.

pitot pressure along the axis of symmetry of an underexpanded jet computed using the method of characteristics¹⁶. The closer-in measurements $X/D < 2$ are affected by the flow through the projectile hole and are lower than the predicted curve. Since the data are not taken on the axis of symmetry, the measured pressures should be lower than comparable axial values. Thus, while the agreement between the two plots may be somewhat fortuitous, it does indicate that after an initial transient period, a quasi-steady flow is established which behaves as an underexpanded jet. Donaldson and Snedeker¹⁷ measure a similar relation between pitot and plate pressures in a study of steady jet impingement. They interpret the pressure difference as due to the greater shock standoff which is associated with the plate flow. Since the measurements indicate the rapid establishment of quasi-steady flow, it is of interest to compare the current data with analytical results.

Smith^{2,3} presents a theory which treats the muzzle flow field as an underexpanded jet. He calculates the efficiency of a given muzzle brake by assuming that the momentum of the propellant gas which would have passed the brake location (if the brake were not present) is transferred to the brake. This permits him to readily account for losses due to the projectile hole and the flow around the brake. He also uses this technique to compute the pressure distribution on brakes with flat surfaces. Since the current brake is flat, direct comparison of the present measurements with Smith's predictions is possible, Figure 10. While not exact, the agreement is reasonable. A portion of the discrepancy may be due to a difference in the ratio of specific heats. Smith uses $\gamma = 1.4$; the propellant gases in the current tests have $\gamma = 1.25$.

The brake force may be expressed as

$$F = \int_A p dA$$

$$= \int_{r_1}^{r_2} p 2\pi r dr.$$

-
16. A. R. Vick, et al, "Comparison of Experimental Free-Jet Boundaries with Theoretical Results Obtained with the Method of Characteristics," NASA, TN D 2327, June 1964.
17. C. D. Donaldson and R. S. Snedeker, "A Study of Free Jet Impingement. Part I. Mean Properties of Free and Impinging Jets," *J. F. M.*, Vol. 45, Part 2., 1971, pp. 281-319.

The integrand of this expression is equivalent to the incremental force added for each increase in brake surface radius. The integrand is plotted versus brake radius in Figure 11. This plot clearly shows the largest increments of brake force are added near $r/D = 0.5$, i.e., the bore radius. This indicates the advantage of minimizing the diameter of the projectile passage.

IV. CONCLUSIONS

Pressure measurements are taken on the surface of a simplistic muzzle brake for a 20mm gun. The data record the variation of pressure with time for the first 400 microseconds after shot ejection. The results indicate that after an initial transient pulse, surface pressures decay to steady state values which agree well with analytical predictions. During the transient period, surface pressures reach levels considerably in excess of steady state values.

ACKNOWLEDGMENTS

The authors are indebted to Mr. D. D. Shear for invaluable assistance in conduct of the experimental program; they thank Mr. D. B. Sleator and Dr. K. S. Fansler for their programming of data read-outs to useful plots.



FIGURE 1a. Photograph of Double Baffle Muzzle Brake for 155mm Gun

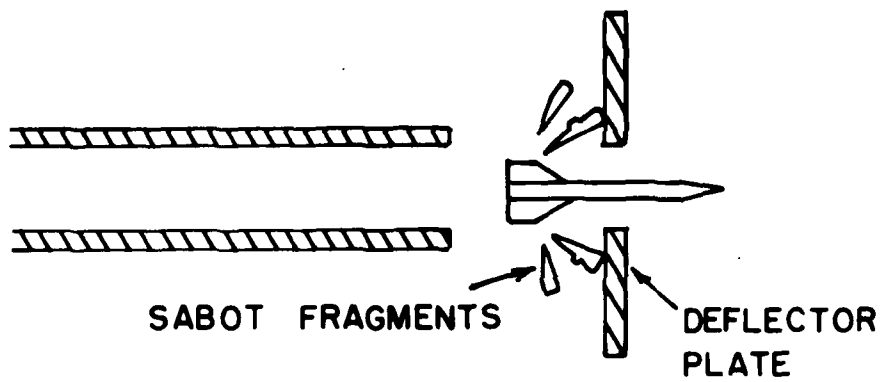


FIGURE 1b. Schematic of Sabot Deflector

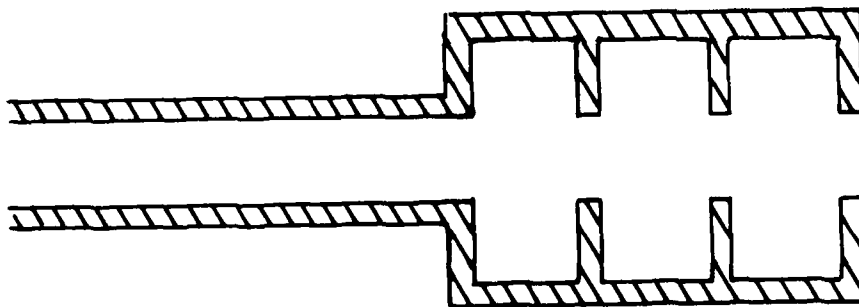


FIGURE 1c. Schematic of Silencer

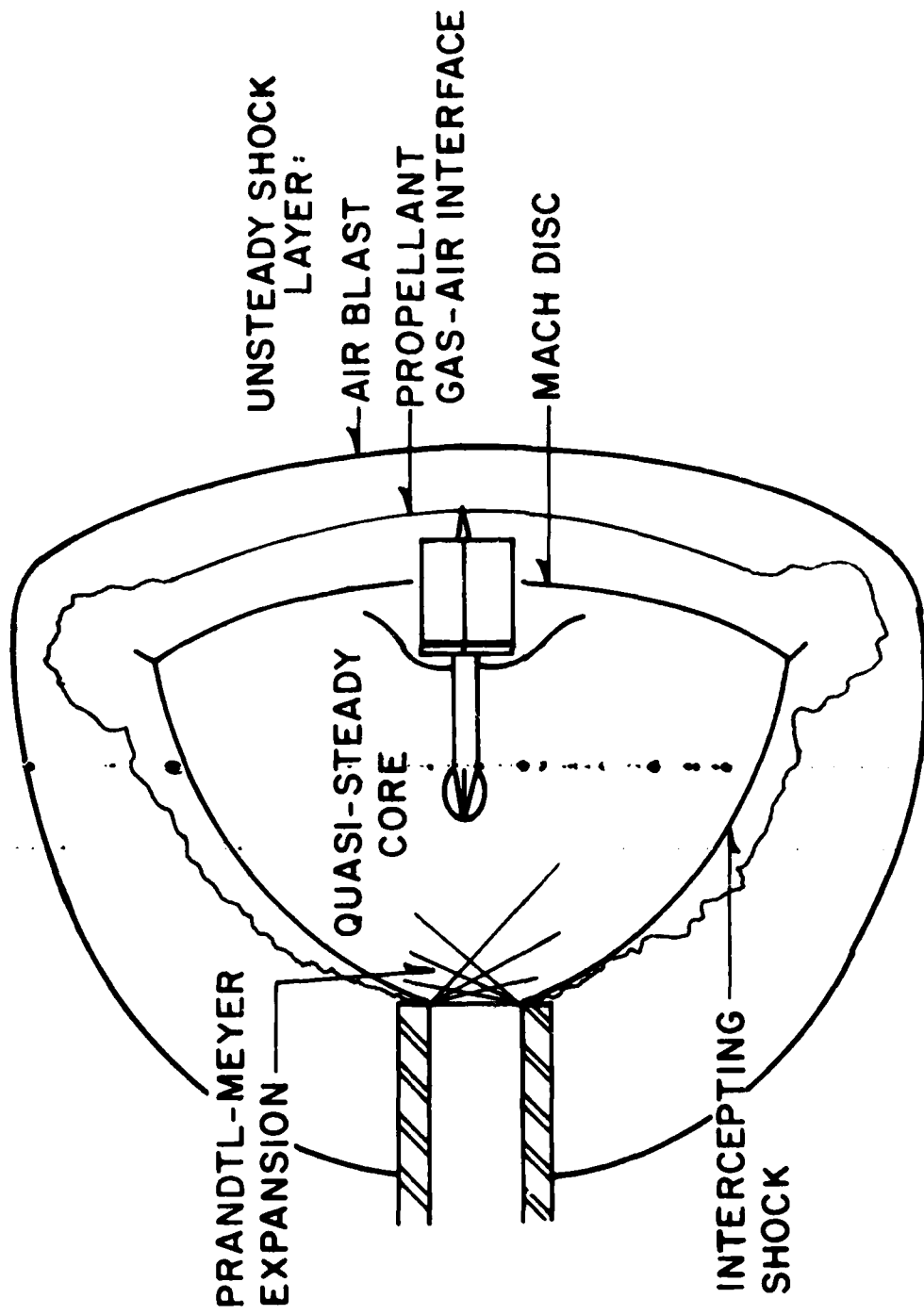
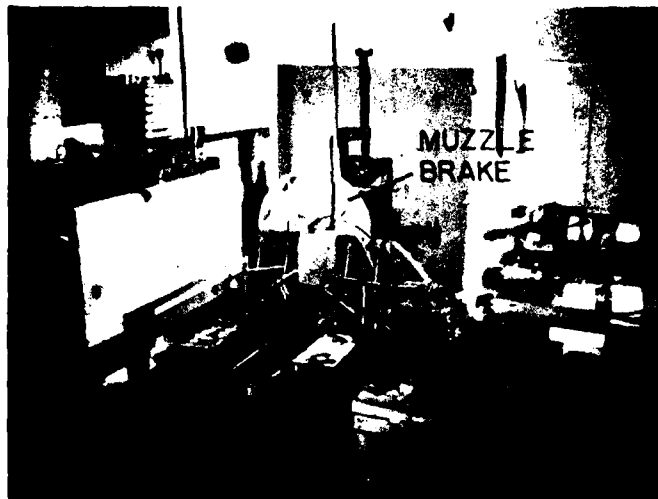
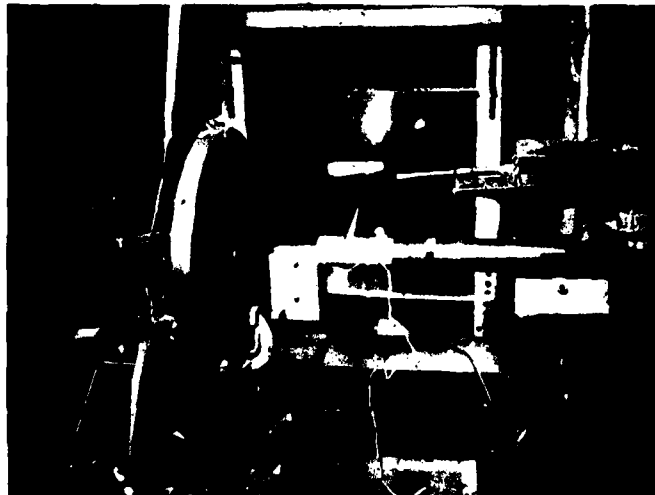


FIGURE 2. Muzzle Flow Field



SPARK LIGHT
SOURCE

X-RAY HEADS



20mm GUN

FIGURE 3. Photographs of Test Set-up

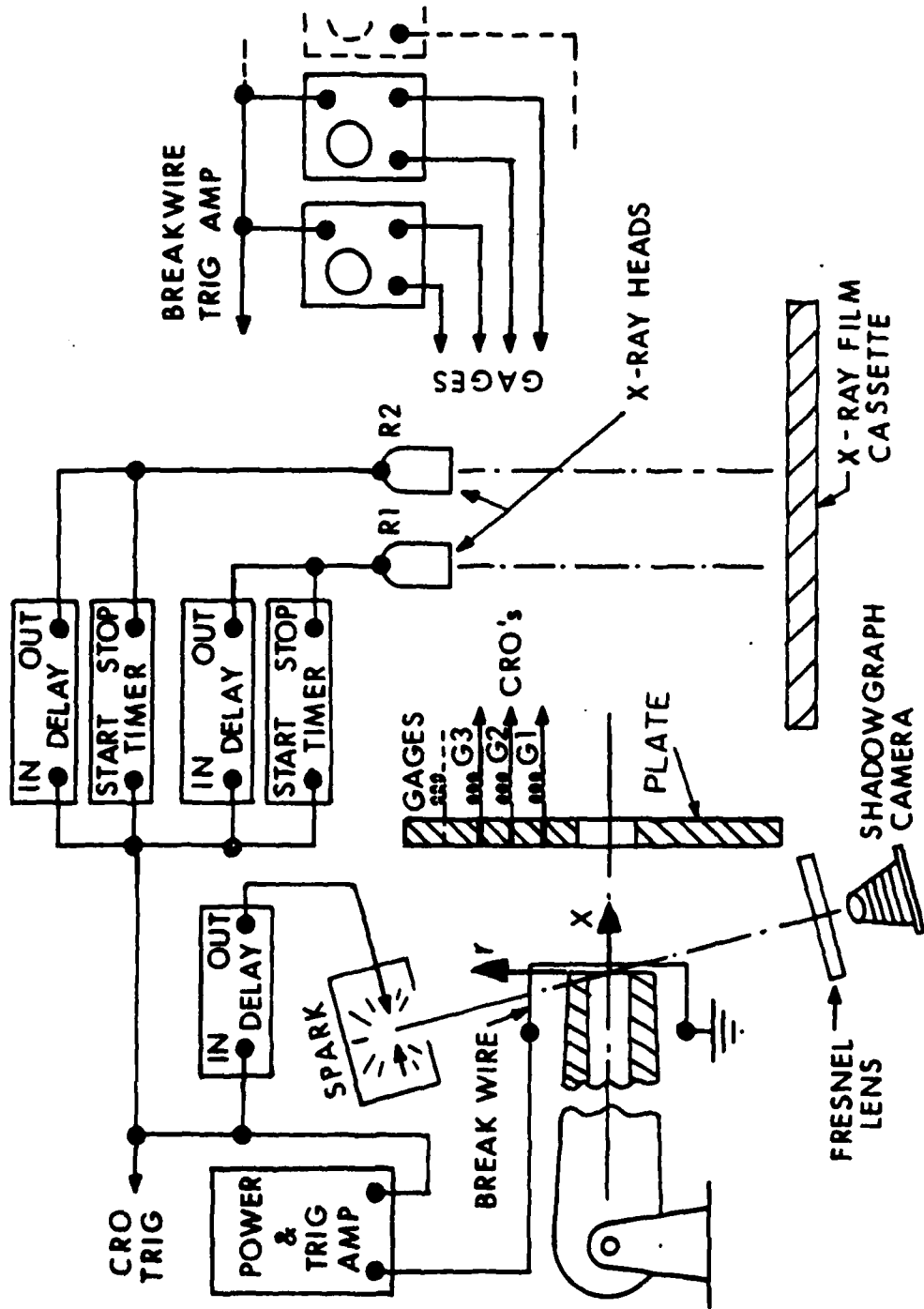


FIGURE 4. Schematic of Test Set-up

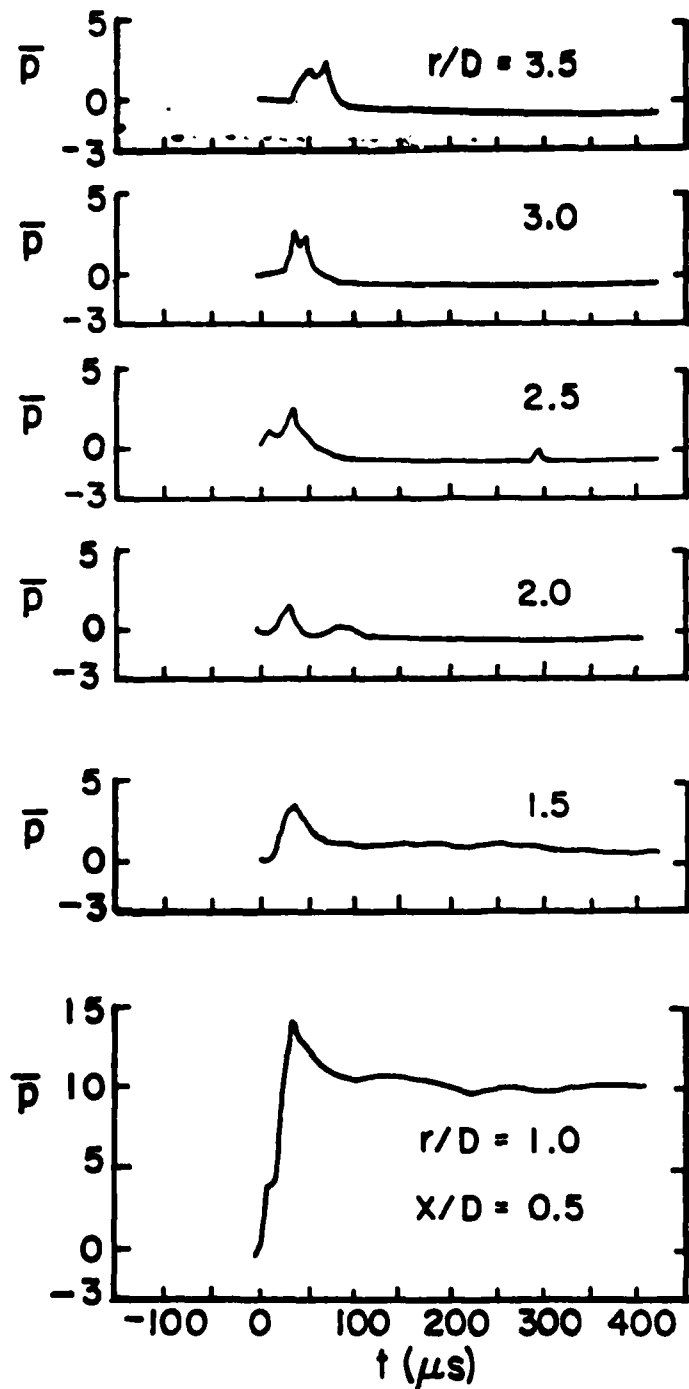


FIGURE 5a. Pressures on Muzzle Brake at Various Radial Locations, $[\bar{p} = (p-p_\infty)/p_\infty]$, for $X/D = 0.5$

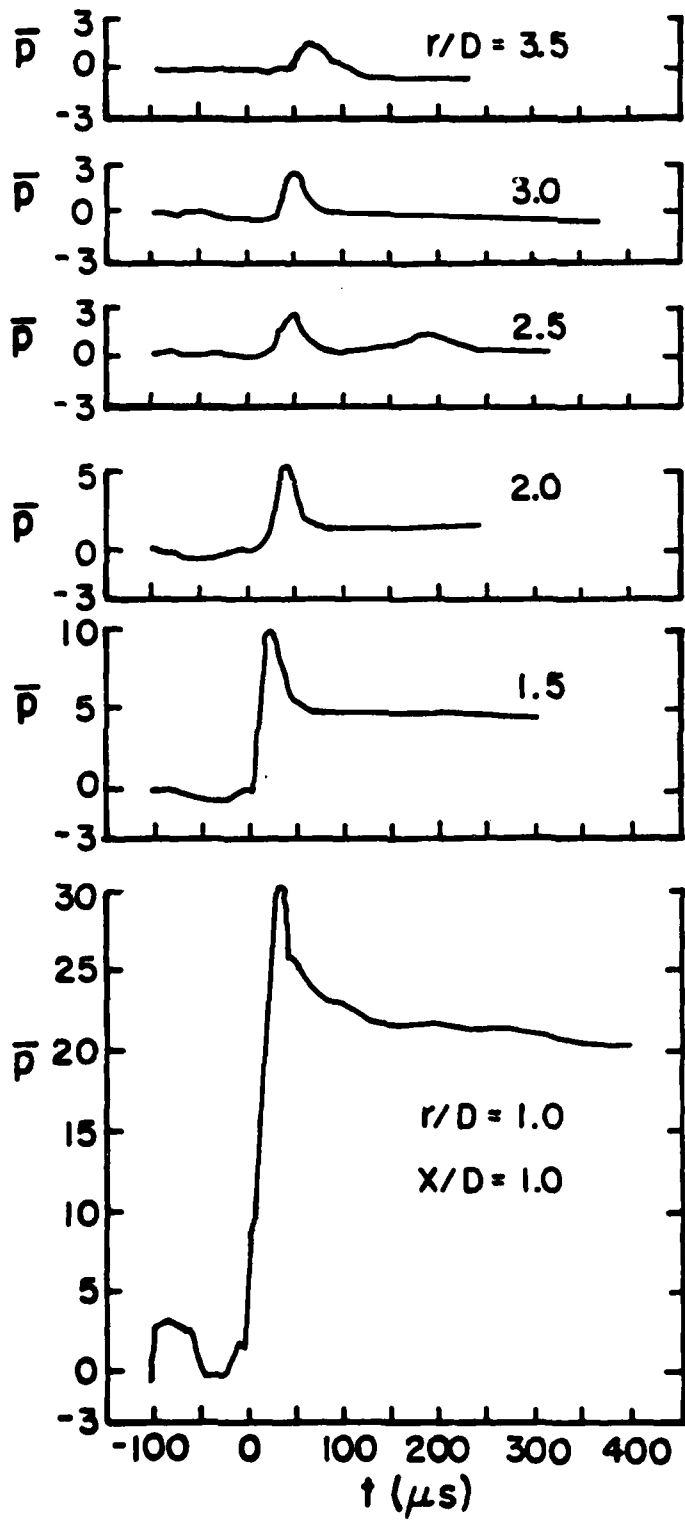


FIGURE 5b. Pressures on Muzzle Brake at Various Radial Locations, $[\bar{p} = (p-p_\infty)/p_\infty]$, for $X/D = 1.0$

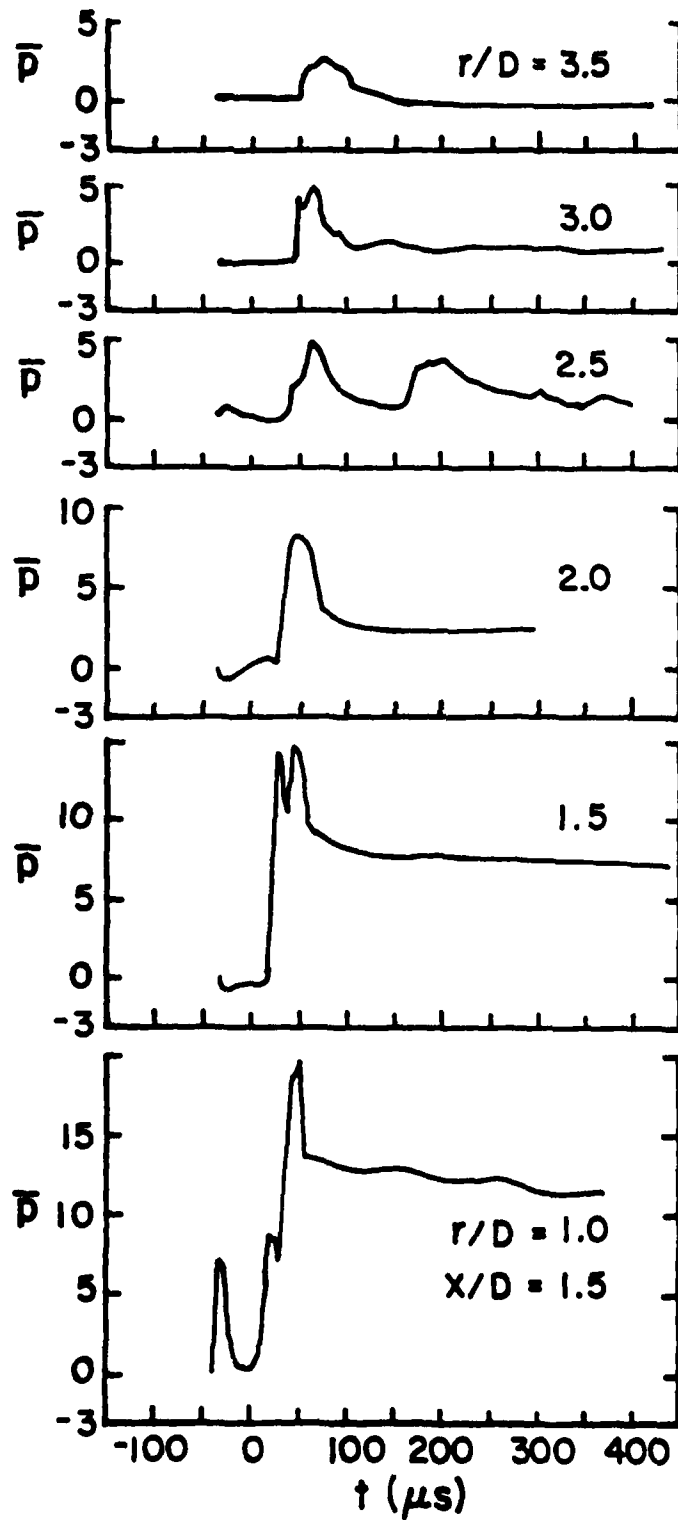


FIGURE 5c. Pressures on Muzzle Brake at Various Radial Locations, $[\bar{p} = (p - p_\infty)/p_\infty]$, for $X/D = 1.5$

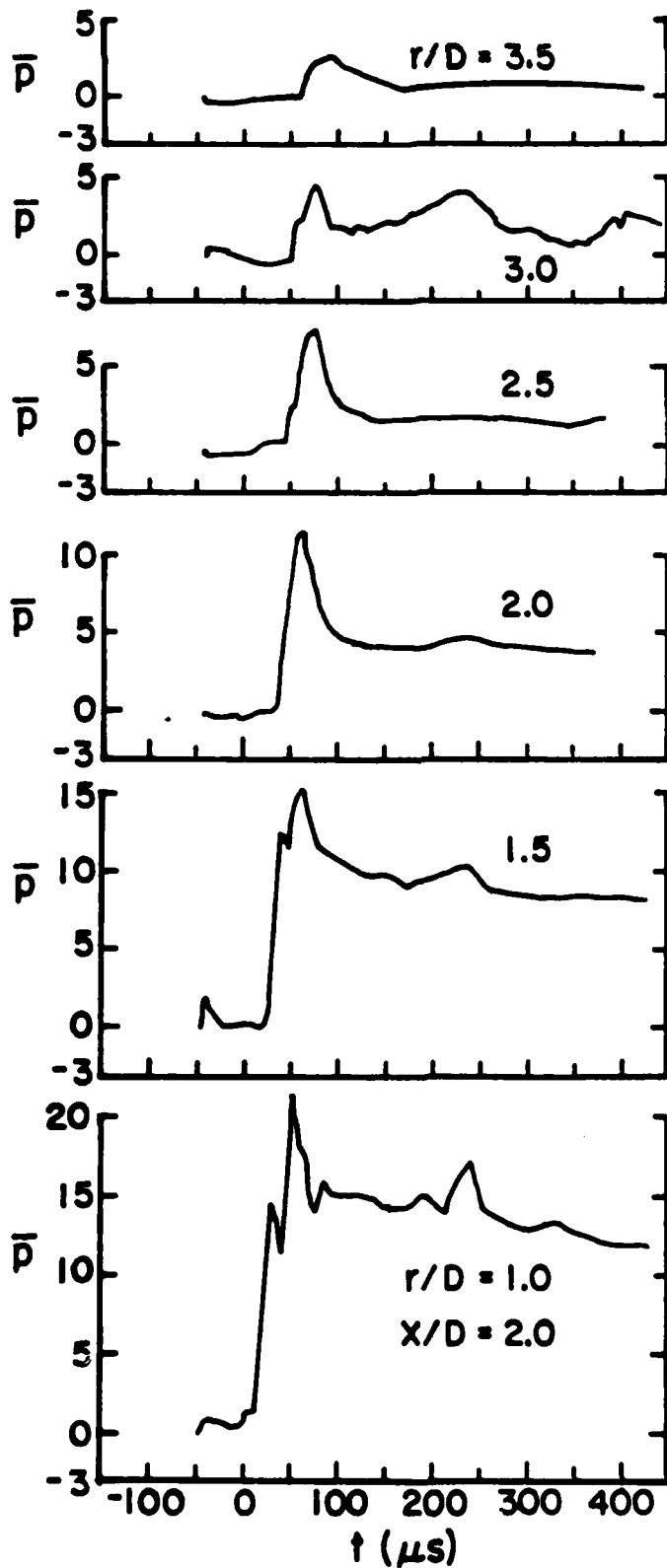


FIGURE 5d. Pressures on Muzzle Brake at Various Radial Locations, $[\bar{p} = (p-p_\infty)/p_\infty]$, for $X/D = 2.0$

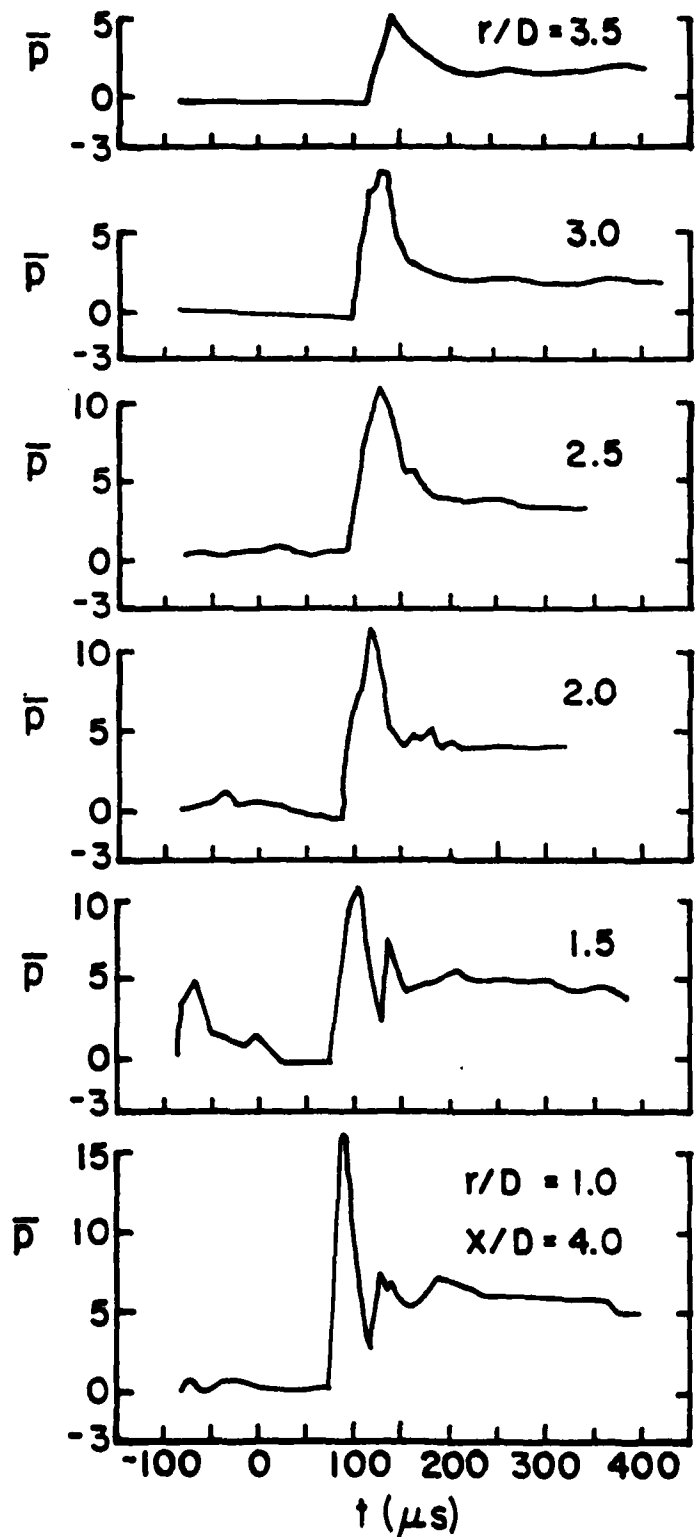


FIGURE 5e. Pressures on Muzzle Brake at Various Radial Locations, $[\bar{p} = (p-p_\infty)/p_\infty]$, for $X/D = 4.0$

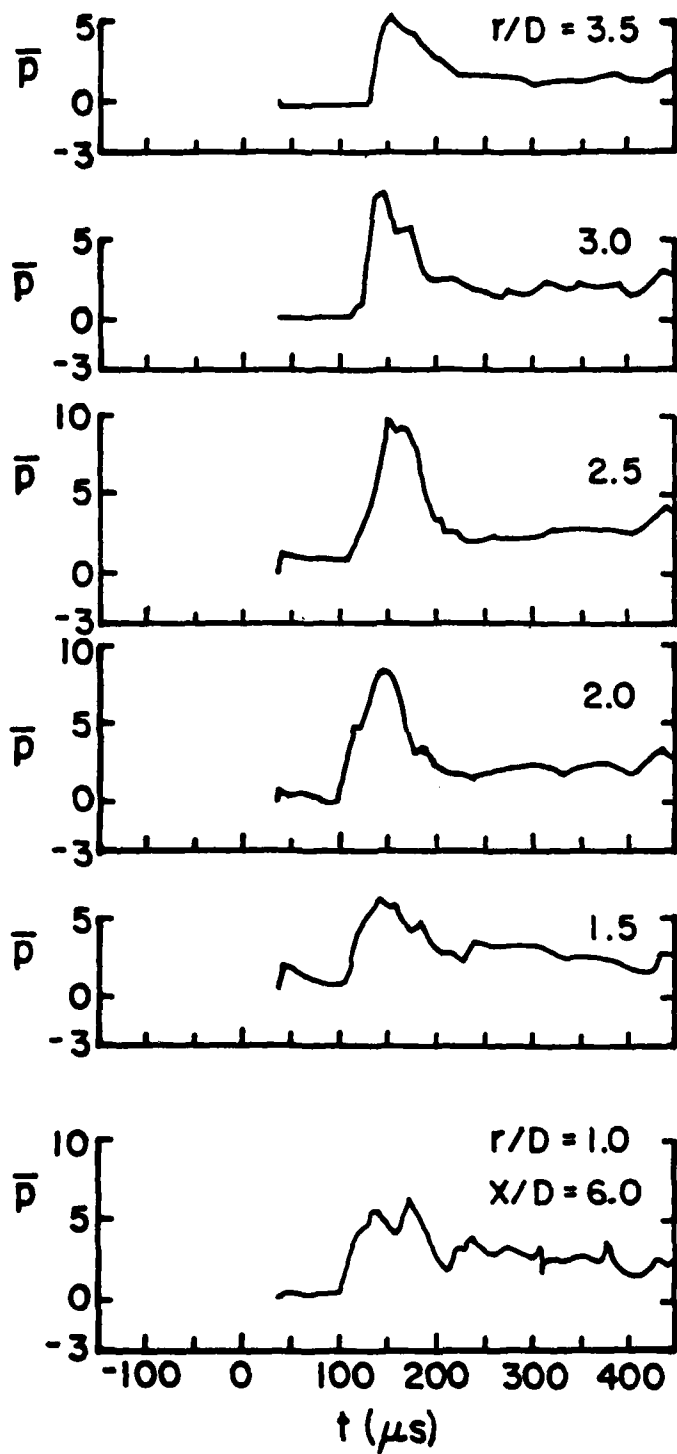


FIGURE 5f. Pressures on Muzzle Brake at Various Radial Locations, $[\bar{p} = (p-p_\infty)/p_\infty]$, for $X/D = 6.0$

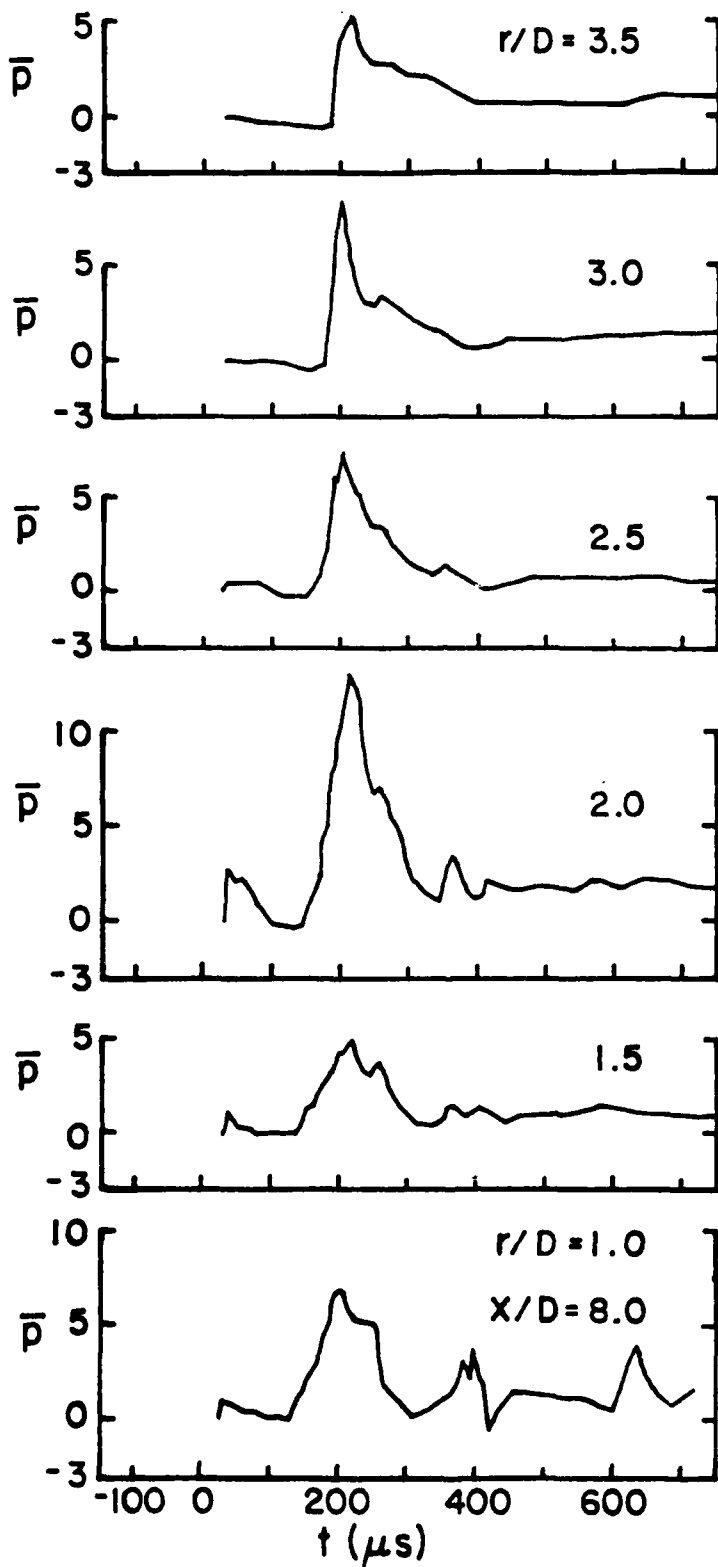


FIGURE 5g. Pressures on Muzzle Brake at Various Radial Locations, $[\bar{p} = (p - p_\infty) / p_\infty]$, for $X/D = 8.0$



FIGURE 6. Spark Shadowgraphs of Flow over Muzzle Brake Located at $X/D = 6.0$



FIGURE 6. Spark Shadowgraphs of Flow over Muzzle Brake Located at $X/D = 6.0$ (Continued)

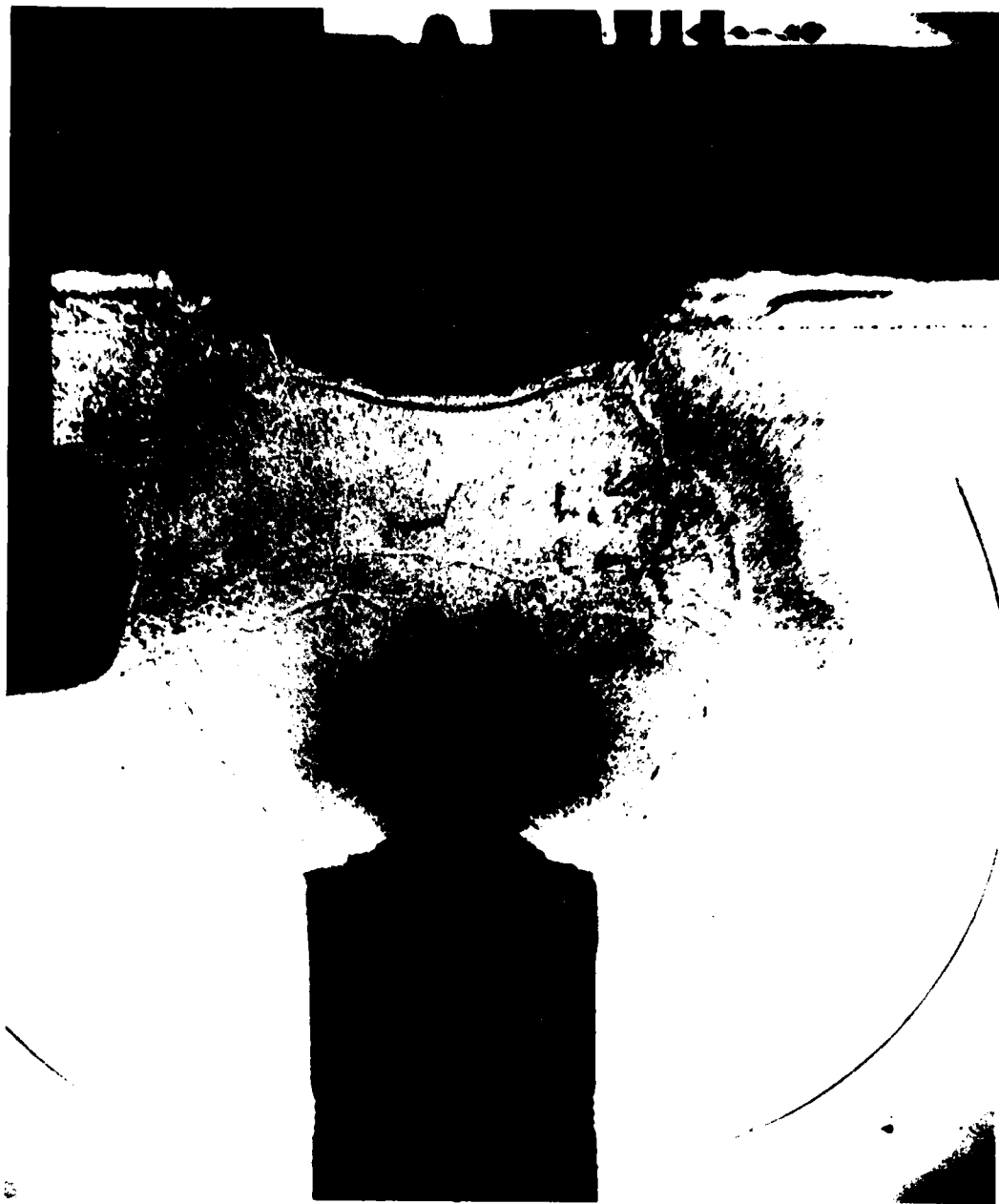


FIGURE 6. Spark Shadowgraphs of Flow over Muzzle Brake Located at $X/D = 6.0$ (Continued)

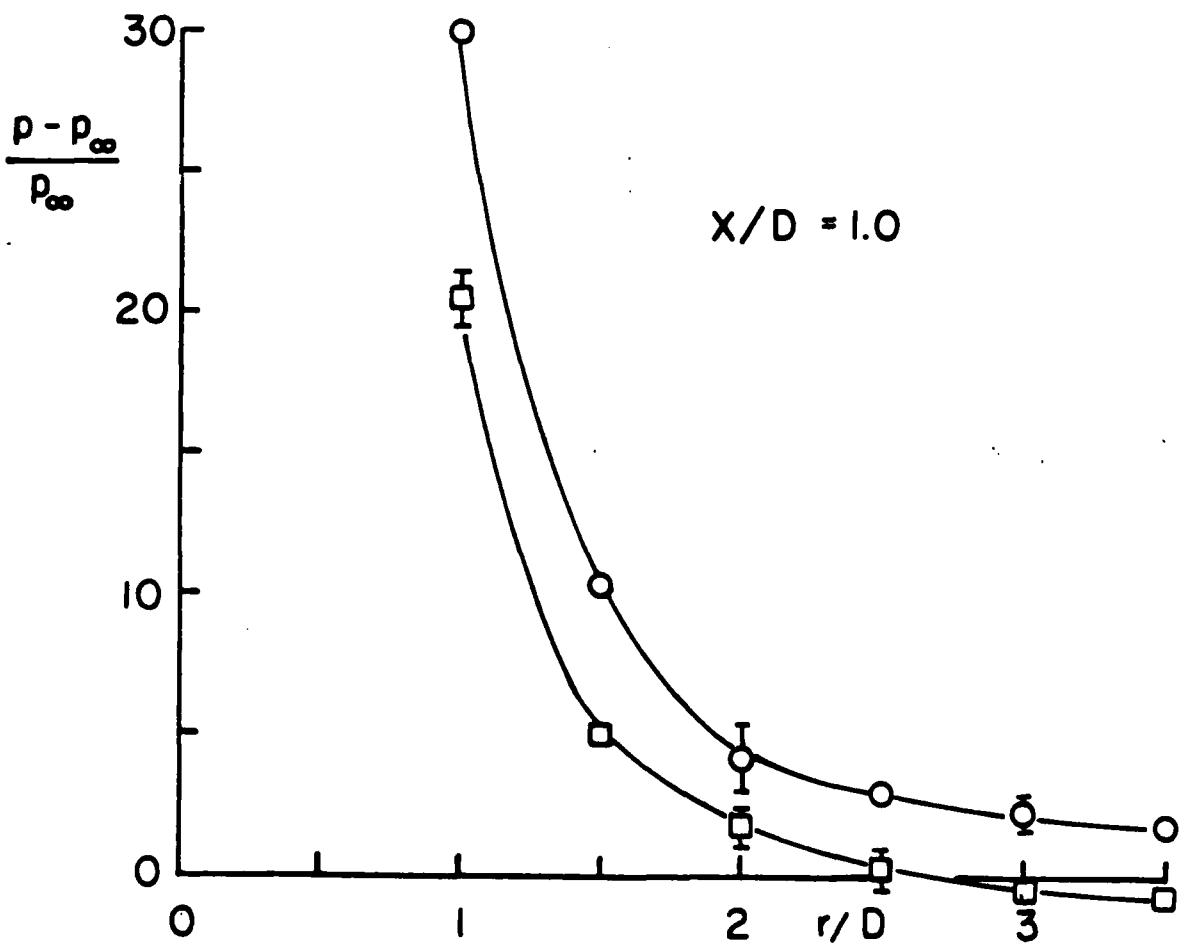
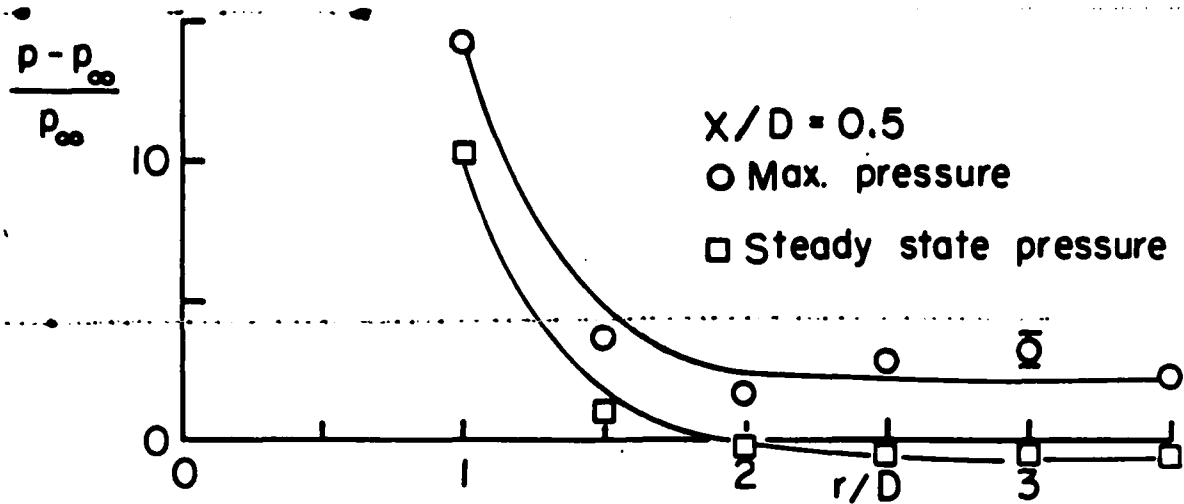


FIGURE 7. Maximum and Steady State Pressures on Muzzle Brake
Surface: a. $X/D = 0.5$, b. $X/D = 1.0$

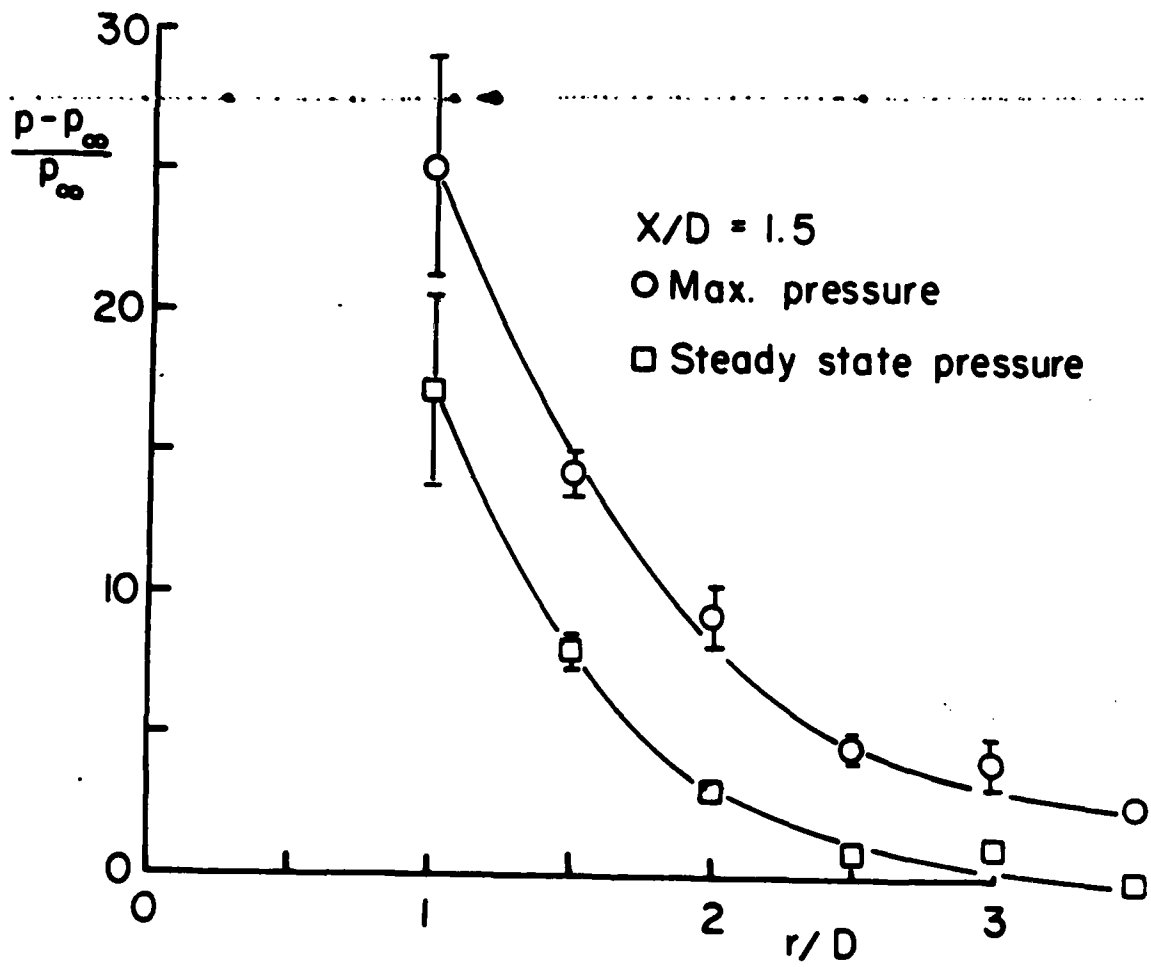


FIGURE 7. Maximum and Steady State Pressures on Muzzle Brake Surface: c. $X/D = 1.5$

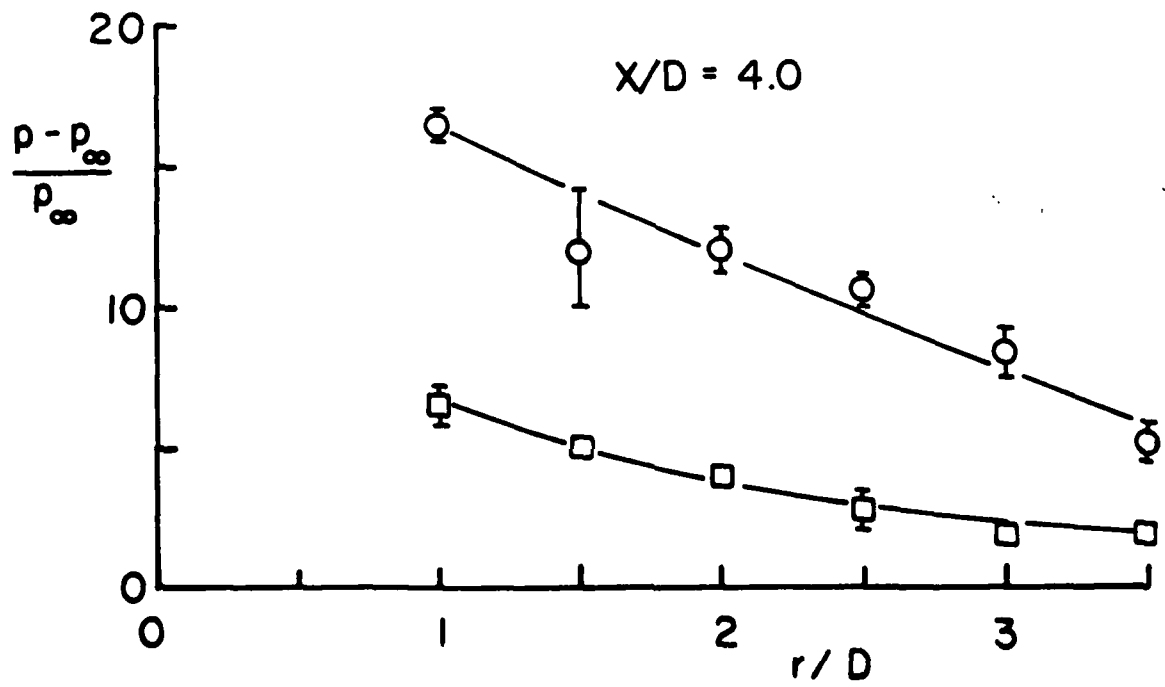
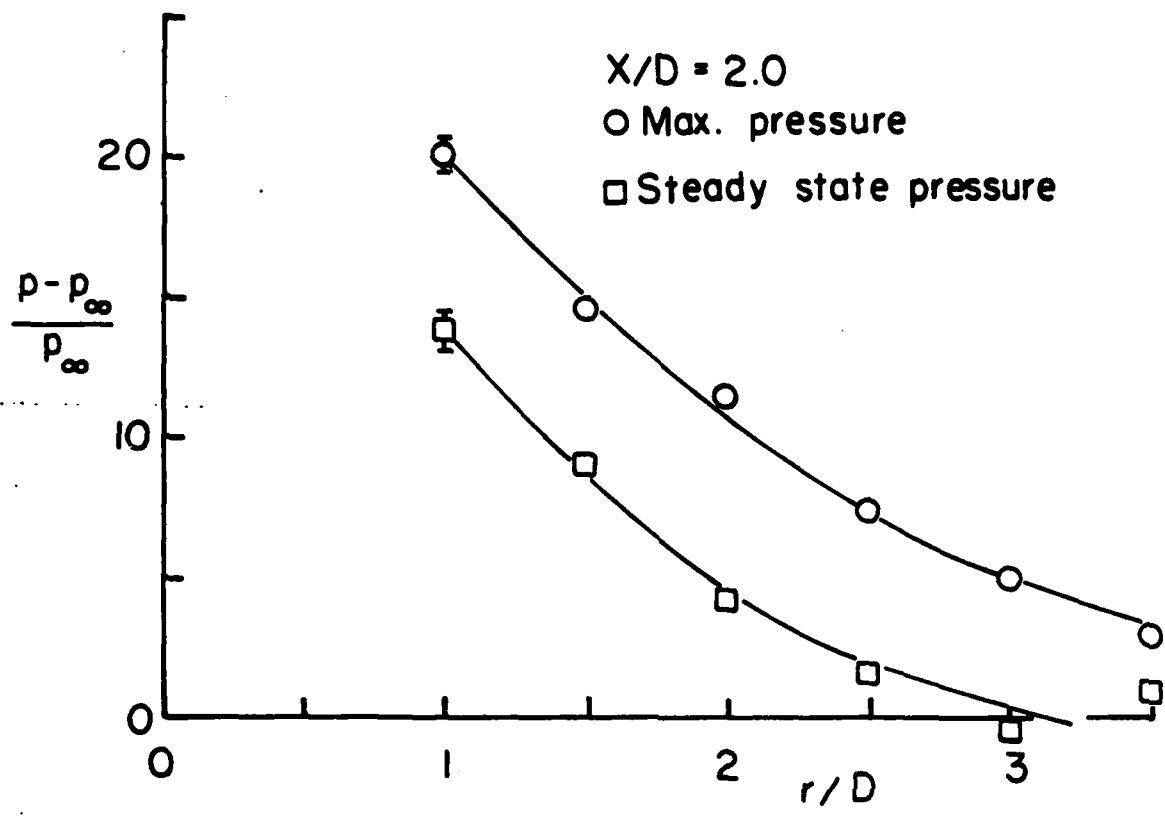


FIGURE 7. Maximum and Steady State Pressures on Muzzle Brake Surface: d. $X/D = 2.0$, e. $X/D = 4.0$

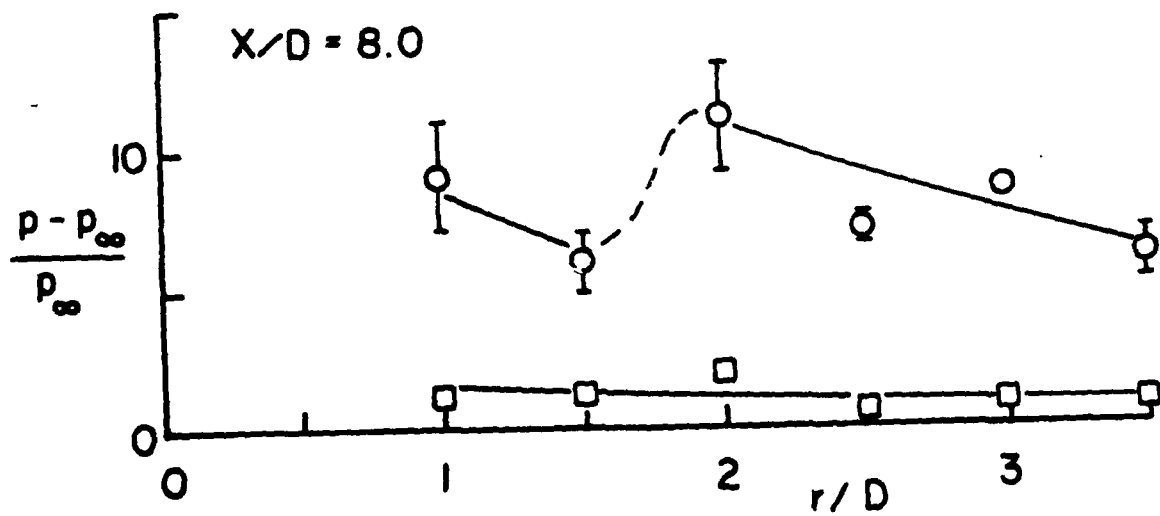
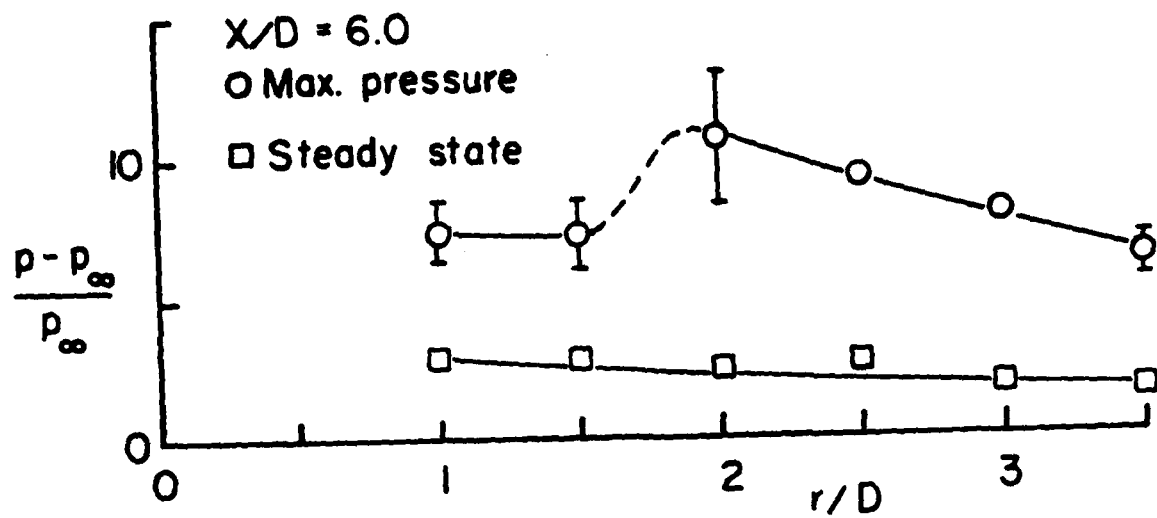
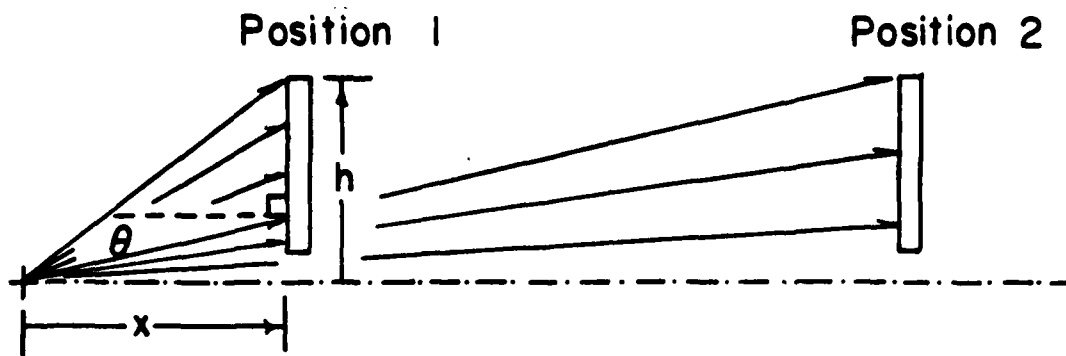


FIGURE 7. Maximum and Steady State Pressures on Muzzle Brake Surface: f. $X/D = 6.0$, g. $X/D = 8.0$



$$\theta_{\max} = \text{Tan}^{-1} (h/x)$$

Therefore:

$$\theta_{\max_1} > \theta_{\max_2}$$

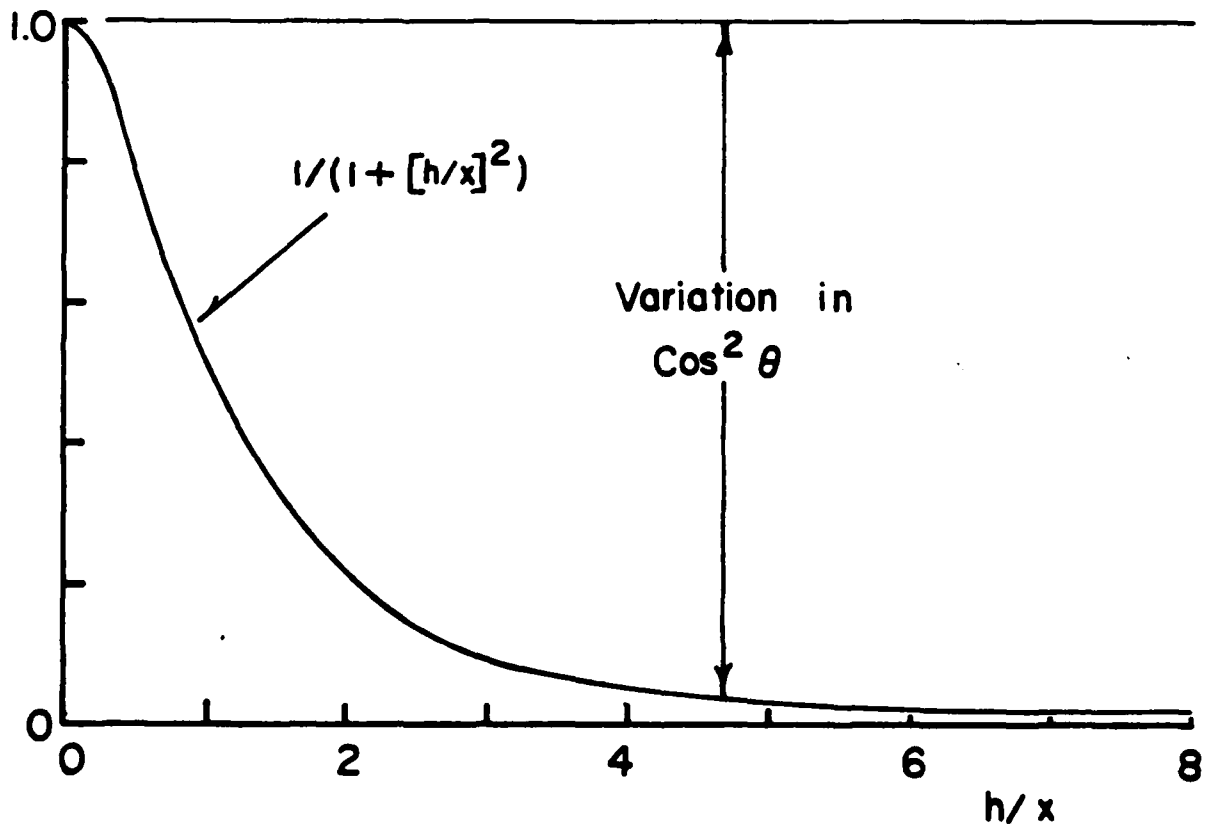


Figure 8. Schematic of Muzzle Brake in a Radial Flow Field

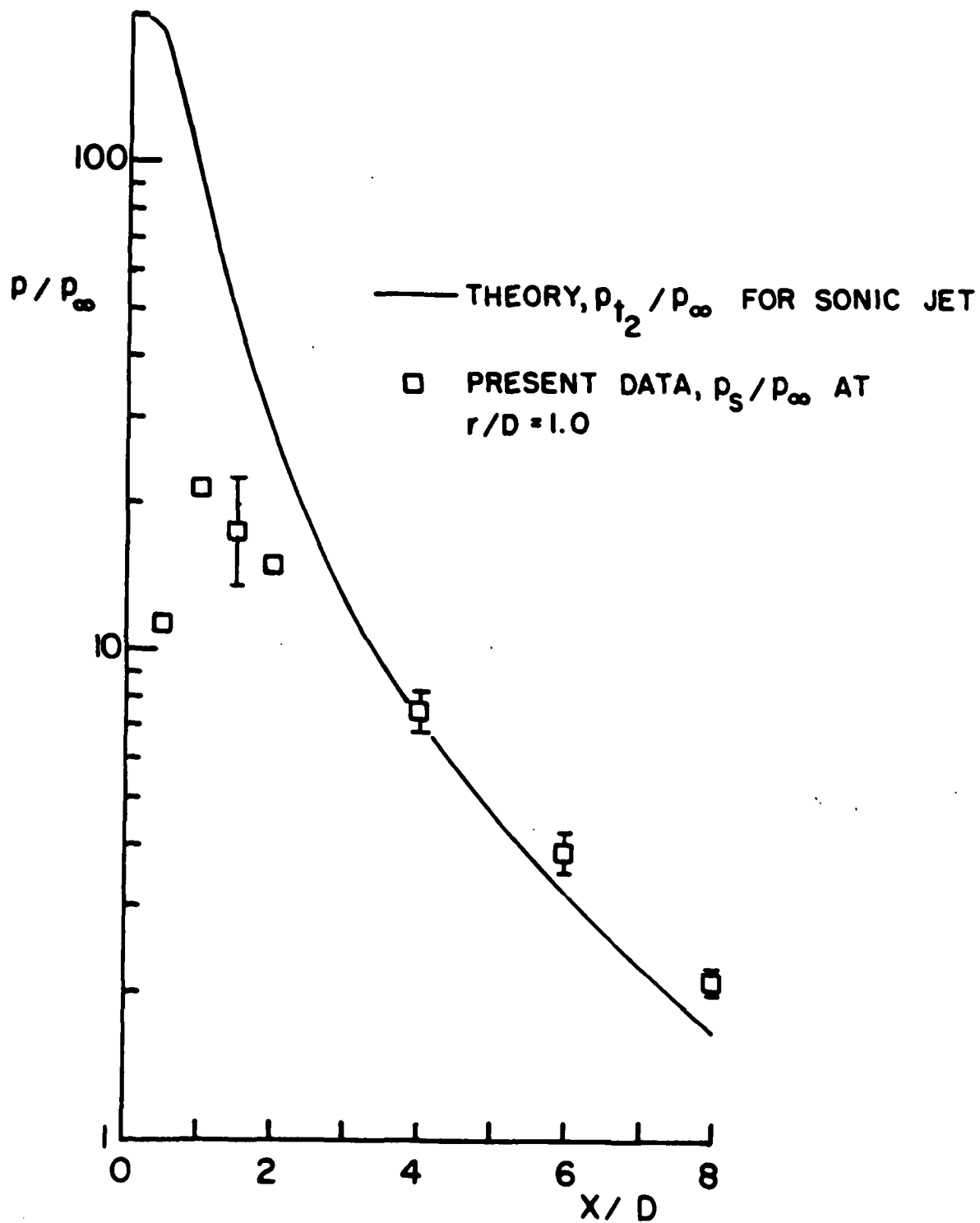


FIGURE 9. Comparison of Steady Jet Theory with Present Data

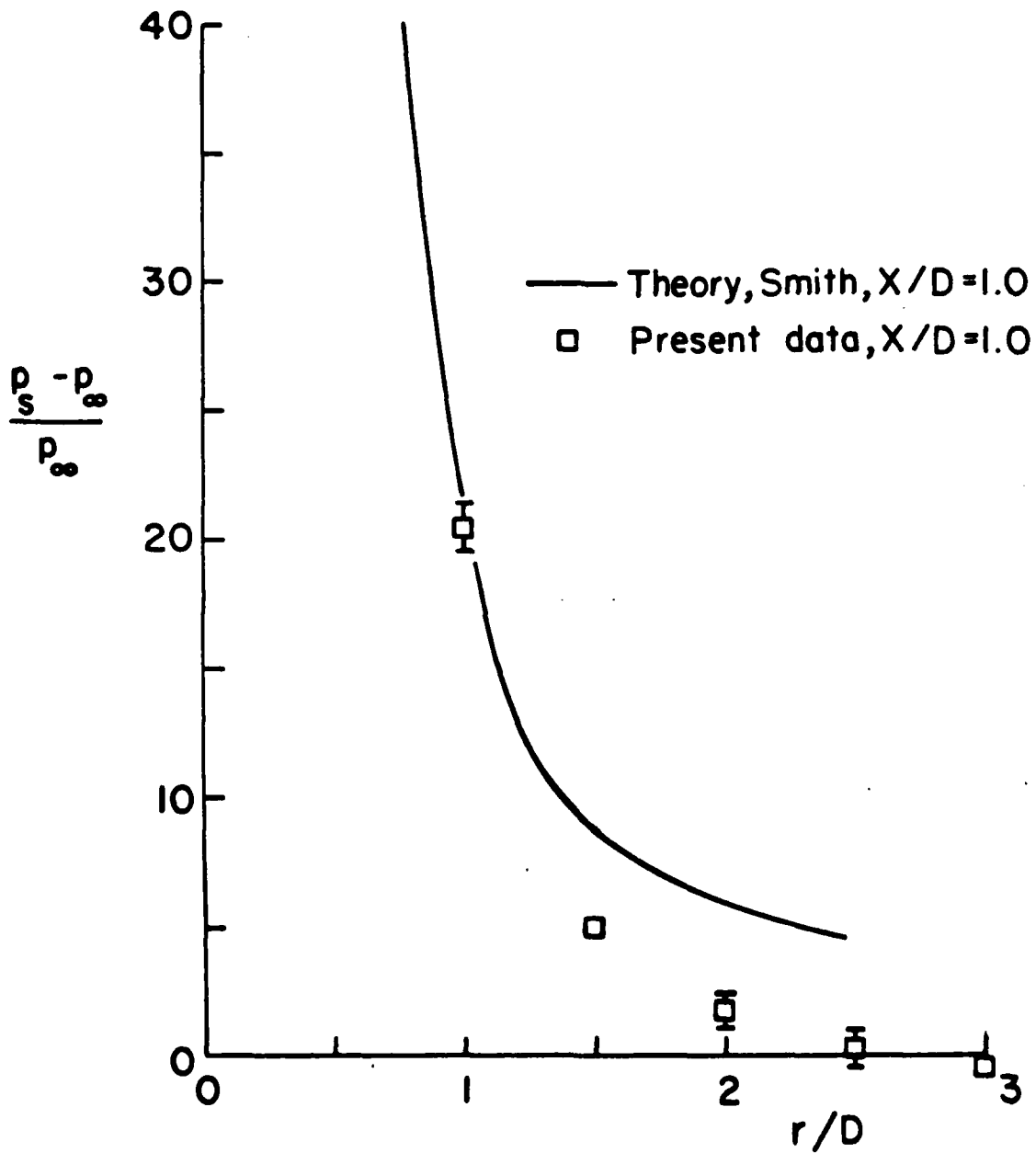


FIGURE 10. Comparison of Surface Pressure Distribution with Theory of Smith

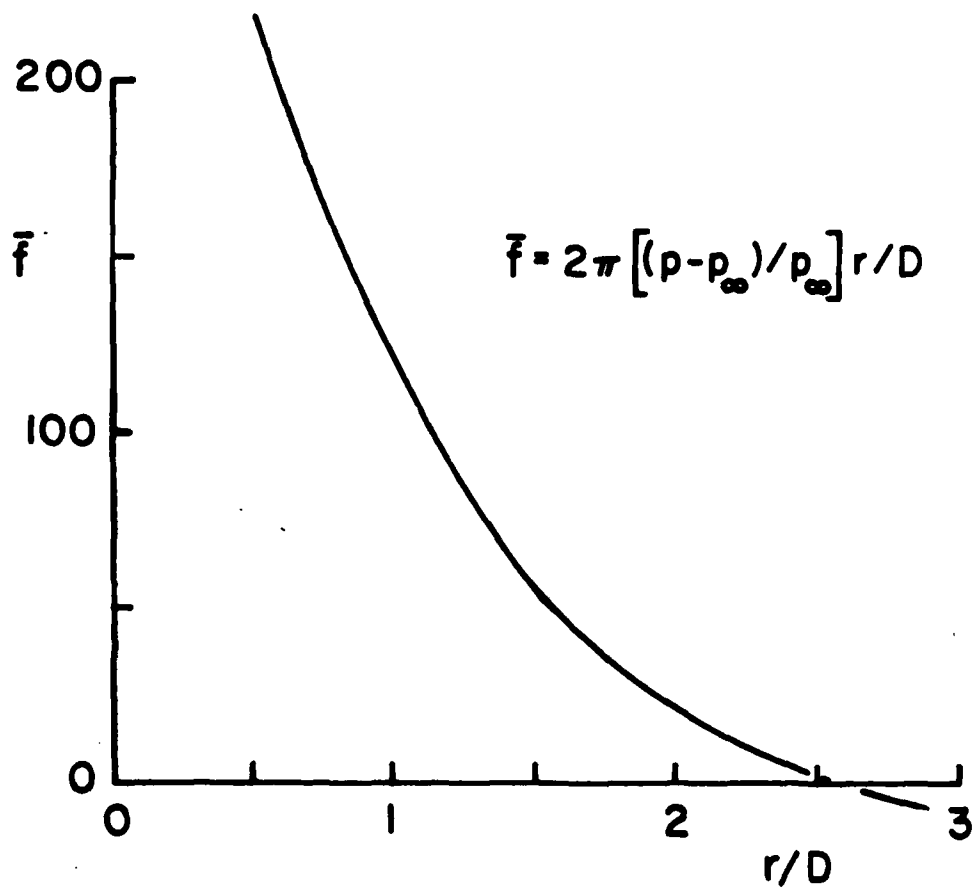


FIGURE 11. Incremental Force Versus Brake Radius for $X/D = 1.0$

REFERENCES

1. K. Oswatitsch, "Flow Research to Improve the Efficiency of Muzzle Brakes, Parts I-III," in Muzzle Brakes, Volume II: Theory, E. Hammer (ed.), Franklin Institute, Philadelphia, 1949.
2. F. Smith, "Model Experiments on Muzzle Brakes," RARDE R 2/66, Royal Armament Research and Development Establishment, Fort Halstead, U.K., 1966. AD 487 121.
3. F. Smith, "Model Experiments on Muzzle Brakes, Part III: Measurement of Pressure Distribution," RARDE R 3/68, Royal Armament Research and Development Establishment, Fort Halstead, U.K., 1968. AD 845 519.
4. E. M. Schmidt and D. D. Shear, "Optical Measurements of Muzzle Blast," AIAA J., Vol. 13, No. 8, August 1975, pp. 1086-1091.
5. K. Oswatitsch, "Intermediate Ballistics," DVL R 358, Deutschen Versuchsanstalt für Luft-und Raumfahrt, Aachen, Germany, June 1964. AD 473 249.
6. R. M. Traci, J. L. Farr, and C. Y. Liu, "A Numerical Method for the Simulation of Muzzle Gas Flows with Fixed and Moving Boundaries," BRL CR 161, U. S. Army Ballistic Research Laboratory, Aberdeen Proving Ground, MD, June 1974. AD784144.
7. F. H. Maille, "Numerical Calculation of a 105mm Gun Blast with Projectile," NWL TR 3002, U. S. Naval Weapons Laboratory, Dahlgren, VA, August 1973. AD 770818.
8. T. D. Taylor, "Calculation of Muzzle Blast Fields," PA R 4155, Picatinny Arsenal, Dover, NJ, December 1970. AD 881 523L.
9. C. K. Zoltani, "Calculation of the Muzzle Flow Field of the 155mm Howitzer M-109," BRL R 1901, U. S. Army Ballistic Research Laboratory, Aberdeen Proving Ground, MD, August 1976. AD B012935L.
10. F. H. Maille, "Finite Difference Calculations of the Free-Air Blast Field About the Muzzle and a Simple Muzzle Brake of a 105mm Howitzer," NWL TR 2938, U. S. Naval Weapons Laboratory, Dahlgren, VA, May 1973.
11. E. M. Schmidt, E. J. Gion, and D. D. Shear, "Acoustic Thermometric Measurements of Propellant Gas Temperatures in Guns," AIAA J., Vol. 15, No. 2, February 1977, pp. 222-226.

REFERENCES (Continued)

12. J. I. Erdos and P. Del Guidice, "Calculation of Muzzle Blast Flow-fields," AIAA J., Vol. 13, No. 8, August 1975, pp. 1048-1055.
13. D. W. Eastman and L. P. Radtke, "Flow Field of an Exhaust Plume Impinging on a Simulated Lunar Surface," AIAA J., Vol. 1, No. 6, June 1963, pp. 1430-1431.
14. J. C. Carling and B. L. Hunt, "The Near Wall Jet of a Normally Impinging, Uniform, Axisymmetric, Supersonic Jet," JFM, Vol. 66, Part 1, 1974, pp. 159-176.
15. S. Hoffman, "Normal Impingement Loads due to Small Air Jets Issuing from a Base Plate," NASA, TN D 6817, June 1972.
16. A. R. Vick, et al, "Comparison of Experimental Free-Jet Boundaries with Theoretical Results Obtained with the Method of Characteristics," NASA, TN D 2327, June 1964.
17. C. D. Donaldson and R. S. Snedeker, "A Study of Free Jet Impingement. Part 1. Mean Properties of Free and Impinging Jets," J. F. M., Vol. 45, Part 2., 1971, pp. 281-319.

LIST OF SYMBOLS

a	speed of sound
A	area
D	diameter of projectile (20mm)
\bar{f}	$2\pi[(p-p_\infty)/p_\infty]r/D$
F	force on muzzle brake
h	radial distance along muzzle brake surface
p	pressure
r	radial coordinate
u	axial velocity
X	axial coordinate
θ	angle between flow velocity vector and surface normal of muzzle brake

Subscripts

m	maximum value
s	steady state value
∞	ambient conditions
1	conditions in propellant gas prior to shot ejection

Superscripts

*	sonic conditions
---	------------------

DISTRIBUTION LIST

<u>No. of Copies</u>	<u>Organization</u>	<u>No. of Copies</u>	<u>Organization</u>
12	Commander Defense Documentation Center ATTN: DDC-TCA Cameron Station Alexandria, VA 22314	1	Commander US Army Jefferson Proving Ground ATTN: STEJP-TD-D Madison, IN 47250
1	Director Defense Nuclear Agency Washington, DC 20305	4	Commander US Army Missile Research and Development Command ATTN: DRDMI-R DRDMI-RBL DRDMI-RDK Mr. R. Becht Mr. R. Deep Redstone Arsenal, AL 35809
1	Commander US Army Materiel Development and Readiness Command ATTN: DRCDMA-ST 5001 Eisenhower Avenue Alexandria, VA 22333	1	Commander US Army Tank Automotive Development Command ATTN: DRDTA-RWL Warren, MI 48090
1	Commander US Army Materiel Development and Readiness Command ATTN: DRCDL 5001 Eisenhower Avenue Alexandria, VA 22333	2	Commander US Army Mobility Equipment Research & Development Command ATTN: Tech Docu Cen, Bldg. 315 DRSME-RZT Fort Belvoir, VA 22060
3	Commander US Army Aviation Systems Command ATTN: DRSAV-E DRSAV-EQA, CPT Schrage DRCPM-AAH, G. Smith 12th and Spruce Streets St. Louis, MO 63166	5	Commander US Army Armament Materiel Readiness Command ATTN: Technical Lib DRSAR-RDG, J. Blick Rock Island, IL 61202
	Director US Army Air Mobility Research and Development Laboratory Ames Research Center Moffett Field, CA 94035	2	Commander US Army Armament Materiel Readiness Command ATTN: Rodman Laboratories S. Thompson S. Burley Rock Island, IL 61202
1	Commander US Army Electronics Command ATTN: DRSEL-RD Fort Monmouth, NJ 07703		

DISTRIBUTION LIST

<u>No. of Copies</u>	<u>Organization</u>	<u>No. of Copies</u>	<u>Organization</u>
5	Commander US Army Armament Research and Development Command ATTN: SARPA-DR-D, S.Wasserman DRDAR-LC-F, Mr. A. Loeb Mr. D. Mertz Mr. F. Friedman SARPA-D, Mr. Lindner Dover, NJ 07801	3	Commander US Army Watervliet Arsenal ATTN: SARWV-PDR-AMM Dr. J. Zweig SARWV-RDD-SE, P.A. Alto DRDAR-LC, G.C. Carofano Watervliet, NY 12189
5	Commander US Army Armament Research and Development Command ATTN: SARPA-V, E. Walbrecht Mr. S. Verner SARPA-VE, Dr. Kaufman SARPA-FR-M-MA Mr. E. Barrieres SARPA-PA-S, W.Dzingala Dover, NJ 07801	2	Commander US Army Harry Diamond Labs ATTN: DRXDO-TI DRXDO-DAB, H.J. Davis 2800 Powder Mill Road Adelphi, MD 20783
5	Commander US Army Frankford Arsenal ATTN: Mr. T. Boldt SARFA-U2100, J.Mitchell SARFA-U3100, S. Fulton SARFA-J7200, S.Goldstein SARFA-L4100-150-2 Mr. C. Sleischer, Jr. Philadelphia, PA 19137	1	Commander US Army Materials and Mechanics Research Center ATTN: DRXMR-ATL Watertown, MA 02172
4	Commander US Army Frankford Arsenal ATTN: SARFA-73300 Mr. S. Hirshman Mr. A. Cianciosi SARFA-MDS-D-220 F. Puzycki C. Rueter Philadelphia, PA 19137	1	Commander US Army Natick Research and Development Command ATTN: DRXRE, Dr. D. Sieling Natick, MA 01762
2	Commander US Army Watervliet Arsenal ATTN: Tech Lib SARWV-PDR-S, F. Sautter Watervliet, NY 12189	1	Director US Army TRADOC Systems Analysis Activity ATTN: ATAA-SA White Sands Missile Range NM 88002
		1	Commander US Army Research Office ATTN: CRD-AA-EH P. O. Box 12211 Research Triangle Park NC 27709
		1	Director US Army BMD Advanced Technology Center P. O. Box 1500, West Station Huntsville, AL 35807

DISTRIBUTION LIST

<u>No. of Copies</u>	<u>Organization</u>	<u>No. of Copies</u>	<u>Organization</u>
1	Commander US Army Ballistic Missile Defense Systems Command Huntsville, AL 35804	3	Commander US Naval Research Laboratory ATTN: Tech Info Div Code 7700, D. A. Kolb Code 7720, Dr. E. McClean Washington, DC 20375
1	Director US Army Advanced Materiel Concepts Agency 5001 Eisenhower Avenue Alexandria, VA 22333	1	Commander US Naval Ordnance Station ATTN: Code FS13A, P. Sewell Indian Head, MD 20640
3	Commander US Naval Air Systems Command ATTN: AIR-604 Washington, DC 20360	1	AFRPL/LKCB, Dr. Horning Edwards AFB, CA 93523
3	Commander US Naval Ordnance Systems Command ATTN: ORD-9132 Washington, DC 20360	2	ADTC/ADBPS-12 Eglin AFB, FL 32542
2	Commander and Director David W. Taylor Naval Ship Research and Development Ctr ATTN: Tech Lib Aerodynamic Lab Bethesda, MD 20084	3	AFATL/DLTL Eglin AFB, FL 32542
3	Commander US Naval Surface Weapons Center ATTN: Code GX, Dr. W. Kemper Mr. F. H. Maille Dr. G. Moore Dahlgren, VA 22448	2	AFATL (DLRA, F. Burgess; Tech Lib) Eglin AFB, FL 32542
3	Commander US Naval Surface Weapons Center ATTN: Code 312, Mr. F. Regan Mr. S. Hastings Code 730, Tech Lib Silver Spring, MD 20910	1	AFWL/DEV Kirtland AFB, NM 87117
1	Commander US Naval Weapons Center ATTN: Code 553, Tech Lib China Lake, CA 93555	1	ASD/XRA (Stinfo) Wright-Patterson AFB, OH 45433
		2	Director National Aeronautics and Space Administration George C. Marshall Space Flight Center ATTN: MS-I, Lib R-AERO-AE, A. Felix Huntsville, AL 35812
		1	Director Jet Propulsion Laboratory ATTN: Tech Lib 2800 Oak Grove Drive Pasadena, CA 91103

DISTRIBUTION LIST

<u>No. of Copies</u>	<u>Organization</u>	<u>No. of Copies</u>	<u>Organization</u>
1	Director National Aeronautics and Space Administration Langley Research Center ATTN: MS 185, Tech Lib Langley Station Hampton, VA 23365	1	Battelle Columbus Laboratories ATTN: J. E. Backofen, Jr. 505 King Avenue Columbus, OH 43201
1	Director NASA Scientific & Technical Information Facility ATTN: SAK/DL P. O. Box 8757 Baltimore/Washington International Airport, MD 21240	1	Technical Director Colt Firearms Corporation 150 Huyshore Avenue Hartford, CT 14061
1	AAI Corporation ATTN: Dr. T. Stastny Cockeysville, MD 21030	1	General Electric Corporation Armaments Division ATTN: Mr. R. Whyte Lakeside Avenue Burlington, VT 05401
1	Advanced Technology Labs ATTN: Dr. J. Erdos Merrick & Steward Avenues Westbury, NY 11590	1	Martin Marietta Aerospace ATTN: Mr. A. J. Culotta P. O. Box 5387 Orlando, FL 32805
1	Aerospace Corporation ATTN: Dr. T. Taylor P. O. Box 92957 Los Angeles, CA 90009	1	Winchester-Western Division Olin Corporation New Haven, CT 06504
2	ARO, Inc. ATTN: Tech Lib Arnold AFS, TN 37389	1	Rockwell Int'l Science Center ATTN: Dr. Norman Malmuth P. O. Box 1085 1000 Oaks, CA 91360
1	ARTEC Associates, Inc. ATTN: Dr. S. Gill 26046 Eden Landing Road Hayward, CA 94545	1	Sandia Laboratories ATTN: Aerodynamics Dept Org 5620, R. Maydew Albuquerque, NM 87115
1	AVCO Systems Division ATTN: Dr. W. Reinecke 201 Lowell Street Wilmington, MA 01887	1	S&D Dynamics, Inc. ATTN: Dr. M. Soifer 755 New York Avenue Huntington, NY 11743
		1	Guggenheim Aeronautical Lab California Institute of Tech ATTN: Tech Lib Pasadena, CA 91104

DISTRIBUTION LIST

<u>No. of Copies</u>	<u>Organization</u>	<u>No. of Copies</u>	<u>Organization</u>
2	Franklin Institute ATTN: Dr. Carfagno Dr. Wachtell Race & 20th Streets Philadelphia, PA 19103	1	Director Forrestal Research Center Princeton University Princeton, NJ 08540
1	Director Applied Physics Laboratory The Johns Hopkins University Johns Hopkins Road Laurel, MD 20810	1	Forrestal Campus Library Princeton University ATTN: Dr. M. Summerfield P. O. Box 710 Princeton, NJ 08540
1	Massachusetts Institute of Technology Dept of Aeronautics and Astronautics ATTN: Tech Lib 77 Massachusetts Avenue Cambridge, MA 02139	1	Southwest Research Institute ATTN: Mr. Peter S. Westine P. O. Drawer 28510 8500 Culebra Road San Antonio, TX 78228
1	Ohio State University Dept of Aeronautics and Astronautical Engineering ATTN: Tech Lib Columbus, OH 43210		<u>Aberdeen Proving Ground</u> Marine Corps Ln Ofc Dir, USAMSAA Cmdr, USA CSL/EA ATTN: A. Flatau, SAREA-DE-W Bldg. E3516
2	Polytechnic Institute of New York Graduate Center ATTN: Tech Lib Dr. G. Moretti Route 110 Farmingdale, NY 11735		